SRC TR 88-103-r1

Performance Comparison Of Different Spread-Spectrum Signaling Schemes For Cellular Mobile Radio Networks

By

M. Soroushnejad
and
E. Geraniotis

PERFORMANCE COMPARISON OF DIFFERENT SPREAD-SPECTRUM SIGNALING SCHEMES FOR CELLULAR MOBILE RADIO NETWORKS

Mohsen Soroushnejad and Evaggelos Geraniotis

Department of Electrical Engineering
and Systems Research Center
University of Maryland
College Park, MD 20742

ABSTRACT

A comparison of different spread-spectrum signaling schemes in a cellular mobile radio network, in terms of throughput and packet error probability is carried out. Bounds on the bit and packet error probabilities are derived for data modulation schemes like binary phase-shift-keying (BPSK) with coherent demodulation and M-ary frequency-shift keying (MFSK) with noncoherent demodulation. Reed-Solomon coding is employed for error-correction purpose. In all cases, the effect of varying interference power (according to some inverse power of distance) of both the desired signal and the other interfering signals and of Rayleigh nonselective channel fading is taken into account accurately.

The throughput in the mobile-to-base transmission mode is then evaluated for the aforementioned data modulation, demodulation, and forward-error-control coding schemes. Our comparison shows that under the varying interference power model, the frequency-hopped scheme performs best among all schemes with the same bandwidth. It was also observed that coding significantly enhances the performance of the above schemes.

This research was supported in part by the Office of Naval Research under contract N00014-86-K-0013 and in part by the Systems Research Center at the University of Maryland, College Park, through the National Science Foundation's Engineering Research Centers Program: NSF CDR 8803012.

I. INTRODUCTION

The general feature of most of the spread-spectrum radio network models proposed to date has been a lack of precision in the characterization of the effects of spread-spectrum techniques on network performance. In particular, for the cellular radio network of [1], which employs frequency-hopped signaling, the model of the spread-spectrum multiple-access interference has not been sufficiently accurate, whereas the model and analysis of that paper have successfully taken into account the effects of varying other-user interference power and channel fading.

On the other hand, the models of [2] take into consideration the frequency-hopped spread-spectrum modulation in a much more accurate way but not the effects of varying received power and fading on the other-user interference. This is due to the upper bound on the conditional probability of error given that one or more hits occurred which is used in [2] and originated in [3].

In this paper, we complement the results of [1]-[2], and [4] by providing a precise characterization of the multi-user interference process for direct-sequence and hybrid (direct-sequence/frequency-hopped) spread-spectrum signaling in cellular mobile radio networks, and compare the performance of these schemes in terms of throughput and packet error probability.

A serious omission of [1], which we remedy here, is the lack of a method for evaluating the packet error probability. In a cellular radio network which employs direct-sequence or hybrid spread-spectrum signaling and forward-error-control coding, the packet error probability (when one or several codewords are transmitted in a packet) becomes an important performance measure. The evaluation of this quantity becomes a difficult task because the interfering signals are present with nonzero probability during all of the bits transmitted in the packet and thus any error events on these bits are strongly correlated. Here, we use the characteristic function methods of [5] and [11] to evaluate the bit error probability exactly, and then utilize the Guassian approximation method, introduced in [7]-[9], along with exponential bounds on error probabilities obtained via Guassian approximation to compute the bit/symbol or packet error probability. The exact evaluation of bit error probability of frequency-hopped systems employing non-coherent BFSK data modulation further completes the analysis in [4]. The use of exponential bounds facilitates the computation of packet error probabilities. Comparison of exact bit error probabilities with the bounds shows that the bounds are bonafide and reasonably tight in most cases of interest. By taking into account the effect of varying received power as a function of distance of mobiles from base station, the near-far problem of spread-spectrum systems was quantified which shows that under this realistic model, the frequency-hopped system performs best among all the SS systems considered in this paper.

This paper is organized as follows: in Section II the basic characteristics of the system and network models are presented. Section III presents the analysis of a cellular network for which direct-sequence (DS) or hybrid (frequency-hopped/direct-sequence) spread-spectrum modulation and BPSK data modulation are employed. For both systems without forward-error control and systems with Reed-Solomon coding, accurate bounds are derived for the average bit and packet error probabilities, as well as the throughput. Varying distances, different received pwers and channel fading are taken into account. In Section IV this is repeated for cellular networks which employ DS or hybrid (FH/DS) SS signaling and M-ary FSK (MFSK) modulation with noncoherent demodulation.

II. SYSTEM AND NETWORK MODELS

Our treatment begins with a discussion of the cellular mobile user model used in [1], modified to the cases of direct-sequence and hybrid spread-spectrum signaling schemes. The number of users in a given area of the plane is modeled as a two-dimensional Poisson process. Transmitter-oriented assignment of signature sequences and/or frequency-hopping patterns characterizes the cells. Each mobile has its own signature sequence and/or frequency-hopping pattern for transmission and reception; the base station has a list of all the patterns and can listen to several of them. We consider the situation when a mobile station has already established communication with the base station (at the center of the cell) and now communicates in the presence of secondary (multiple-access) interference from other mobile stations. Slotted systems are consisdered and it is assumed that the different users can synchronize their transmissions at the packet level but not necessarily at the bit or dwell time level.

When BPSK with coherent demodulation and DS/SS or hybrid FH-DS/SS signaling is employed, the output of the receiver matched to the i-th mobile station is given by:

$$Z_i = \sqrt{\frac{P_0 g(|0M_i|)}{8}} T \cdot X_i + \sum_{k \neq i} \sqrt{\frac{P_0 g(|0M_k|)}{8}} T \cdot X_k \cdot I_{k,i} + \eta \qquad (1)$$

and is compared to a zero threshold to decide if an 1 or a -1 was sent. In (1), P_0 denotes the transmitted power, common to all mobile stations, T the duration of each data bit and η a zero-mean Gaussian random variable with variance $\frac{N_0 T}{16}$, where $\frac{N_0}{2}$ is the two-sided spectral density of AWGN. When fading is not present, X_k=1. For Rayleigh nonselective fading X_k's, for k=1,2,..., are independent identically distributed Rayleigh random variables with variance 1. The other-user interference term, $I_{k,i}$, is described in detail in [5] for DS/SS systems with deterministic signature sequencesd, [6] for DS/SS systems with random sequences, and [7] for hybrid FH-DS/SS systems. Finally, the function $g(r)$ denotes the attenuation of the signal as a function of the distance between the transmitter and the receiver at the base station. In this paper, we model the cell area as a circular region of plane with radius R, and therefore define $g(r)$ as

$$g(r) = \begin{cases} r_0^{-\alpha}; & 0 \le r \le r_0 \\ r^{-\alpha}; & r_0 \le r \le R \end{cases} \tag{2}$$

where $\alpha = 3.5$. $|0M_i|$ and $|0M_k|$ represent the distances of the mobiles M_i and M_k from the base station 0; R denotes the radius of the circular cell and r_0 is a small fraction of R (e.g., $r_0 = .01R$). It is used to prevent $g(r)$ from taking very large values for r very close to 0. Eq. (1) is equivalent

$$\tilde{Z}_i = X_i + \sum_{k \ne i} \sqrt{\frac{g(|0M_k|)}{g(|0M_i|)}} \cdot X_k \cdot I_{k,i} + \tilde{\eta} \tag{3}$$

where $\tilde{\eta}$ is zero-mean Gaussian with variance $\left[\frac{2E_{b,0}}{N_0} g(|0M_i|)\right]^{-1}$ and $I_{k,i}$ is given in [5], [6], and [7].

Similarly when MFSK with noncoherent demodulation is employed, the output of the in-phase component of the m-th branch (m=1,2, . . . ,M) is given by:

$$Z_{c,m}^{(i)} = \sqrt{\frac{P_0 g(|0M_i|)}{8}} T_s X_i \cos\theta_{i,m} + \sum_{k \ne i} \sqrt{\frac{P_0 g(|0M_k|)}{8}} T_s X_k I_{c,m}^{(k,i)} + \eta_{c,m} \tag{4}$$

where T_s is the duration of each M-ary symbol ($T_s = T\log_2 M$), $\theta_{i,m}$ is uniformly distributed in [0,2π], the other-user interference term $I_{c,m}^{(k,i)}$ is given in [9], and $\eta_{c,m}$ is a zero-mean Gaussian random variable with variance $\frac{N_0 T}{16}$. Eq. (4) is equivalent to

$$\tilde{Z}_{c,m}^{(i)} = X_i \cos\theta_{i,m} + \sum_{k \ne i} \sqrt{\frac{g(|0M_k|)}{g(|0M_i|)}} \cdot X_k \cdot I_{c,m}^{(k,i)} + \tilde{n}_{c,m} \tag{5}$$

where $\tilde{n}_{c,m}$ is zero-mean Gaussian with variance $\left[\frac{2E_{b,0}\log_2 M}{N_0} g(|OM_i|)\right]^{-1}$. The output of the quadrature component of the m-th branch $\tilde{Z}_{s,m}^{(i)}$ can be obtained from (5) by replacing cos(.) with sin(.).

The mobiles M_k are Poisson distributed on a region A of the plane with area S. Let $\{A_j\}_{j=1}^{J}$ be a partition of this region for which all the points (mobile stations) of A_j have the same distance r_j from the origin (base station). Let S_j denote the area of A_j and K_j the number of mobile stations in A_j. It is assumed that K_j is Poisson distributed with probability mass function (pmf)

$$P(K_j = k) = \frac{(\lambda S_j)^k}{k!}\ , \quad k = 0,1,2,... \quad ; \tag{6}$$

so that the average number of mobile stations in A_j is given by $\overline{K}_j = \lambda S_j$; λ denotes the average number of mobiles per unit area. Let $\overline{K} = \sum_{j=1}^{n} \overline{K}_j$ denote the total average number of users in the whole region A; obviously $\overline{K} = \lambda S$. This model is essential to our analysis and enables us to derive closed-form expressions for bit and packet error probabilities.

Let $\tilde{r} = |OM_i|$ be the distance of the mobile M_i (source of the desired signal) from the base station. Notice that through (3) and (5), the sufficient statistic depends on $g(r)$. It turns out that the bit and packet error probabilities for the various systems considered in this paper are concave functions of $g(\tilde{r})$ in part of range of $\tilde{r}$. In this range, we apply Jensen's inequality (to bit error probabilities, for example), in order to obtain

$$E\{P_b[g(\tilde{r})]\} \le P_b[E\{g(\tilde{r})\}]\ . \tag{7}$$

In the range of $\tilde{r}$ in which the function P_b is not concave in $\tilde{r}$, we use $P_b[E\{g(\tilde{r})\}]$ as an approximation. In (7) E denotes expectation with respect to the mobile M_i being uniformly distributed on the region A above (that is, the probability of M_i being in A_j--defined above--is

S_j/S). In the sequel we will be using $E\{g(\tilde{r})\}$ instead of $g(\tilde{r})$ in all our formulas. In particular for a circular region A with radius R we have

$$E\{g(r)\} = \int_0^R \frac{2r}{R^2} g(r) dr = \frac{r_0^{2-\alpha}}{R^2} + \frac{2}{(\alpha-2)R^2}\left[r_0^{2-\alpha} - R^{2-\alpha}\right] = g(\bar{r}) \tag{8}$$

where $\bar{r} = \left[E\{g(r)\}\right]^{-\frac{1}{\alpha}}$. This means that $\bar{r}$ is the value such that an average value of $g(\tilde{r})$ is obtained. Finally, it is convenient to define the ratio $g(|OM_k|)/g(|OM_i|) = g(r)/g(\tilde{r})$, when $g(\tilde{r})$ is replaced by $g(\bar{r})$ as

$$\bar{g}(r) = \frac{g(r)}{g(\bar{r})} = \begin{cases} \left[\dfrac{r_0}{\bar{r}}\right]^{-\alpha}; & 0 \le r \le r_0 \\ \left[\dfrac{r}{\bar{r}}\right]^{-\alpha}; & r_0 \le r \le R \end{cases} \tag{9}$$

III. CELLULAR RADIO NETWORKS WITH COHERENT DS/SS OR FH-DS/SS SIGNALING

A. Systems Without Forward-Error-Control

For systems employing BPSK with coherent demodulation, asynchronous users (at the chip or bit level), over an **AWGN channel** starting point is the following expression for the **bit error probabillity:**

$$P_b = Q\left[\sqrt{\frac{2E_{b,0}}{N_0}g(\overline{r})}\right]+\frac{1}{\pi}\int_0^{\infty}\frac{\sin u}{u}\exp\left\{-\frac{N_0u^2}{4E_{b,0}\,g(\overline{r})}\right\}\left[1-\Phi(u)\right]du\ . \qquad (10)$$

In (10) $Q(x)=\frac{1}{2}erfc\left[\frac{x}{\sqrt{2}}\right]$ is the complementary error function, $\Phi(u)$ is the characteristic function of the other-user interference, and $g(\overline{r})$ is the average attenuation factor for the desired signal. Eq. (10) is derived in [5] for DS/SS systems and corresponds to equation (3). If K denotes the number of interfering users, $\Phi(u)$ takes the form (see [7] for hybrid FH-DS systems and [6] for DS/SS systems):

$$\Phi(u)=\left[\frac{1}{2}\right]^{N-1}\sum_{n=0}^{N-1}\left[\begin{matrix}N-1\\ n\end{matrix}\right]\left[P_h\Phi_{N,n}(u)+1-P_h\right]^K \qquad (11)$$

Eq. (11) holds for hybrid FH-DS/SS systems and is valid under the assumption of equal received power for all signals. It is also assumed that only full hits occur (this gives a slightly pessimistic result). In (11) N is the number of chips per bit, $P_h = \left[1+\frac{1}{N_b}\right]\frac{1}{q}$ is the probability of a hit, N_b is the number of bits per dwell-time (hop), and q is the number of frequencies available for hopping. For DS/SS systems set P_h=1 in (11).

In (11) $\Phi_{N,n}(u)$ for n=0,1, . . . ,$N-1$ is given by

$$\Phi_{N,n}(u)=\frac{4}{\pi T_c}\int_0^{\frac{\pi}{2}}\int_0^{T_c/2}\cos\left\{\frac{u}{N}\frac{R_\psi(\tau)}{T_c}\cos\theta\right\}\cos\left\{\frac{u}{N}\frac{\hat{R}_\psi(\tau)}{T_c}\cos\theta\right\}$$

$$\cos^n\left\{\frac{u}{N}\frac{R_\psi(\tau)+\hat{R}_\psi(\tau)}{T_c}\cos\theta\right\}\cos^{N-1-n}\left\{\frac{u}{N}\frac{R_\psi(\tau)-\hat{R}_\psi(\tau)}{T_c}\cos\theta\right\}d\tau d\theta$$

where $T=NT_c$, for rectangular chip waveforms the partial autocorrelation functions are given by $R_\psi(\tau)=\tau$, $\hat{R}_\psi(\tau)=T_c-\tau$.

For the network model of Section II, $\left[P_h\Phi_{N,n}(u)+1-P_h\right]^K$ of (11) should be replaced by

$$\prod_{j=1}^{J}\left[P_h\Phi_{N,n}\left[u\sqrt{\bar{g}_j}\right]+1-P_h\right]^{K_j} \quad ;$$

Since there are now J groups of K_j users each, all with distance from the origin r_j and normalized attenuation factor $\bar{g}_j$ defined by $\bar{g}_j=\bar{g}(r_j)$.

Next we evaluate the expectation with respect to $\underline{K}=(K_1,K_2,\ldots,K_J)$:

$$E_{\underline{K}}\left\{\prod_{j=1}^{J}\left[P_h\Phi_{N,n}\left[u\sqrt{\bar{g}_j}\right]+1-P_h\right]^{K_j}\right\}=$$

$$=\prod_{j=1}^{J}\left\{\sum_{K_j=0}^{\infty}\frac{(\lambda S_j)^{K_j}}{K_j!}e^{-\lambda S_j}\left[P_h\Phi_{N,n}\left[u\sqrt{\bar{g}_j}\right]+1-P_h\right]^{K_j}\right\}$$

$$=e^{\lambda\sum_{j=1}^{J}S_j P_h\left[\Phi_{N,n}\left[u\sqrt{\bar{g}_j}\right]-1\right]} \qquad (12)$$

Therefore, upon substitution in (11) we obtain

$$\Phi(u)=\left[\frac{1}{2}\right]^{N-1}\sum_{n=0}^{N-1}\binom{N-1}{n}e^{\lambda\sum_{j=1}^{J}S_jP_h\left[\Phi_{N,n}\left[u\sqrt{\bar{g}_j}\right]-1\right]} \qquad (13)$$

Finally, if we let S_j , $j=1,2,\ldots J$ as $J\rightarrow\infty$ cover the circular region, which is centered at 0 and has radius R, then S_j should be replaced by $2\pi r dr$, r_j by r, and the summation by the integral $\int_0^R$. The final result becomes

$$\Phi(u) = \left(\frac{1}{2}\right)^{N-1} \sum_{n=0}^{N-1} \binom{N-1}{n} e^{\lambda \int_0^R 2\pi r \, P_h \left[\Phi_{N,n}\left(u\sqrt{g(r)}\right)-1\right] dr} \tag{14}$$

The average bit error probability can be then obtained from (10) and (14).

When Rayleigh nonselective fading is present (10) should be replaced by

$$P_b = \frac{1}{2}\left\{1 - \left[1 + \left(\frac{\overline{E}_b}{N_0} g(\overline{r})\right)^{-1}\right]^{-\frac{1}{2}}\right\}$$

$$+ \frac{1}{\pi}\int_0^\infty \exp\left\{-\left[1 + \frac{N_0}{\overline{E}_{b,0} g(\overline{r})}\right]\frac{u^2}{4}\right\}\left[1 - \Phi(u)\right] du \ , \tag{15}$$

where $\Phi(u)$ is now given by

$$\Phi(u) = \left(\frac{1}{2}\right)^{N-1} \sum_{n=0}^{N-1} \binom{N-1}{n} \exp\left\{\lambda \int_0^R 2\pi r P_h \left[\int_0^\infty \Phi_{N,n}\left(u\sqrt{g(\overline{r})x}\right) e^{-x} dx - 1\right] dr\right\}. \tag{16}$$

In (15), $\overline{E}_{b,0} = \overline{P}_0 T$ denotes the received energy per bit of the desired signal in the presence of Rayleigh fading and no attenuation (see eq. (3)).

The expressions in (10), (14) and (15)-(16) provide P_b with any desirable accuracy (see details in [4] for similar expressions involving the characteristic function of the other-user interference). However, we can obtain accurate approximations to P_b and more important, to the packet error probability P_E, which require less computational effort than (10) or (15) does. Next, we describe a technique for approximating P_b and P_E efficiently.

Using the extended Gaussian approximation technique of [7], we may approximate the random variable $\tilde{Z}_i$ by a guassian random variable with the same second-order moments which results in the conditional probability of error in an **AWGN** environment given by

$$\tilde{P_b}=Q\left\{\left[\left[\frac{2E_{b,0}}{N_0}g(\bar{r})\right]^{-1}+\frac{m_\psi}{N}\sum_{j=1}^{J}\bar{g}(r_j)k_j\right]^{-1/2}\right\} , \tag{17}$$

where we have conditioned on the fact that k_j users (out of K_j present in the region A_j) cause full hits. At this point we use the exponential bound on $Q(.)$ function which is given by

$$Q(x) \leq \frac{1}{2}e^{-x^2/2} \leq \frac{1}{2}(1-e^{-1/x^2}) \qquad x \geq 0 , \tag{18}$$

to bound $\tilde{P_c} = 1-\tilde{P_b}$, the probability of correct reception of a bit, as

$$\tilde{P_c} = 1-Q\left[\frac{1}{\sqrt{x}}\right] \geq \frac{1}{2}+\frac{1}{2}e^{-x} \tag{19}$$

where x denotes the expression inside [ ] in (17). Figure 1. illustrates this bound. The tighter bound obtained numerically is also shown in this Figure. More generally, one may use an n-term sum of exponentials $\sum_{l=1}^{n} c_l\, e^{\delta_l x}$, to bound $\tilde{P}_c$. The constants c_l and δ_l may be found using any suitable curve-fitting method [10]. We have found 3-term exponential sums to bound $\tilde{P}_c$ for the case of Rayleigh fading and M-ary FSK systems. The exponential bounding enables us to obtain closed form expressions for the packet error probability. Going back to (19), Define

$$\tilde{c_l} = c_l \exp\left\{\delta_l \left[\frac{2E_{b,0}}{N_0}g(\bar{r})\right]^{-1}\right\} \quad l=1,2 , \tag{20}$$

$$\tilde{g}(r) = \frac{m_\psi}{N}\bar{g}(r) , \tag{21}$$

and

$$\tilde{g_j} = \tilde{g}(r_j). \tag{22}$$

Here, $c_1=c_2=\frac{1}{2}$, and $\delta_1=0,\delta_2=-1$. In (21) $m_\psi = 1/3$ for a rectangular chip waveform and $m_\psi = \frac{15+2\pi^2}{12\pi^2}$ for a sine chip waveform. We now evaluate the average of the expression in (19) with respect to the binomial distribution of hits (each with probability P_h) and the Poisson distribution on the K_j's [see (6)]. The computation is as follows:

$$E_{\underline{K}}\{E_h\{\tilde{P_c}\}\} = E_{\underline{K}}\left\{\prod_{j=1}^{J} \sum_{k_j=0}^{K_j} \begin{bmatrix} K_j \\ k_j \end{bmatrix} P_h^{k_j} \left[1-P_h\right]^{K_j-k_j} \sum_{l=1}^{2} \tilde{c_l} e^{\delta_l \sum_{j=1}^{J} \bar{g}_j k_j}\right\} ,$$

$$= \sum_{l=1}^{2} \tilde{c_l} E_{\underline{K}} \left\{\prod_{j=1}^{J} \left[P_h e^{\delta_l \cdot \bar{g}_j} + 1-P_h\right]^{K_j}\right\} ,$$

$$= \sum_{l=1}^{2} \tilde{c_l} \left\{\prod_{j=1}^{J} \sum_{K_j=0}^{\infty} \frac{(\lambda S_j)^{K_j}}{K_j!} e^{-\lambda S_j} \left[P_h e^{\delta_l \cdot \bar{g}_j} + 1-P_h\right]^{K_j}\right\} .$$

Finally, we have

$$E_{\underline{K}}\{E_h\{\tilde{P_c}\}\} = \sum_{l=1}^{2} \tilde{c_l}\ e^{\lambda \sum_{j=1}^{J} S_j \left[P_h \left(e^{\delta_l \bar{g}_j} - 1\right)\right]} \tag{23}$$

For the special case of a circular region of radius R we obtain

$$P_b = 1-\sum_{l=1}^{2} \tilde{c_l} e^{\lambda \int_0^R 2\pi r \left[P_h \left(e^{\delta_l \bar{g}(r)} - 1\right)\right] dr} \tag{24}$$

Similarly, when **Rayleigh nonselective fading** is present, (17) should be replaced by

$$\tilde{P_b} = \frac{1}{2}\left\{1-\left[1+\left[\frac{\bar{E}_0}{N_0}\right]^{-1} + \frac{m_\Psi}{N}\sum_{j=1}^{J} \bar{g}(r_j)k_j\right]^{-1/2}\right\}, \tag{25}$$

(19) should be replaced by

$$\tilde{P_c} = 1-\frac{1}{2}\left[1 - \frac{1}{\sqrt{1+x}}\right] \geq \sum_{l=1}^{3} c_l e^{\delta_l x} \ ;\ x \geq 0 \ , \tag{26}$$

and P_b is still given by (24), where now

$$\tilde{c}_l = c_l \exp\left\{\delta_l \left[\frac{\bar{E}_{b,0}}{N_0} g(\bar{r})\right]^{-1}\right\}, \tag{27}$$

and c_l, δ_l for $l = 1,2,3$ have been obtained numerically and given in Appendix.

The results above hold for hybrid FH-DS/SS systems. It suffices to set $P_h=1$ to obtain the corresponding results for DS/SS systems and $N=1$ to obtain the results for FH/SS (purely frequency-hopped) systems.

To evaluate P_E, the **packet error probability** for uncoded systems, we write $P_C = 1-P_E$ as

$$P_C = E_K\left\{E_h\left\{\left[1-\tilde{P}_b\right]^L\right\}\right\} \tag{28}$$

where L is the number of bits per packet, $\tilde{P}_b$ is the conditional error probability defined in (17), and E_h and E_K denote the expectations with respect to the distribution of hits and the number of users in each subregion A_j [refer to the paragraph between eq. (19) and (20)]. In writing (28) we assumed that given $(k_1, k_2, \ldots, k_J)$ (the number of users in each subregion which cause full hits), bit errors are independent within the packet; when interleaving is not used this is only an approximation for DS/SS systems without which no explicit results can be obtained; for hybrid FH-DS/SS systems it is a rather realistic assumption.

If we use the bound in (19) for $1-\tilde{P}_b = \tilde{P}_c$ we obtain

$$\tilde{P}_c^{\,L} = \sum_{i=0}^{L}\binom{L}{i}\tilde{c}_1^{\,i}\tilde{c}_2^{\,L-i}\cdot e^{[\delta_1 i+\delta_2(L-i)]\sum_{j=1}^{J}\tilde{g}_j k_j} \tag{29}$$

Therefore, after evaluating the expectations in the same way we derived (23), we obtain

$$P_C = E_K\left\{E_h\{\tilde{P}_c^{\,L}\}\right\} = \sum_{i=0}^{L}\binom{L}{i}\tilde{c}_1^{\,i}\tilde{c}_2^{\,L-i}\cdot e^{\lambda\sum_{j=1}^{J}S_j\left[P_h\left(e^{[\delta_1 i+\delta_2(L-i)]\tilde{g}_j}-1\right)\right]dr}, \tag{30}$$

and for a circular disk of radius R

$$P_C = F(L) = \sum_{i=0}^{L}\binom{L}{i}\tilde{c}_1^{\,i}\tilde{c}_2^{\,L-i}\cdot e^{\lambda\int_0^R 2\pi r\left[P_h\left(e^{[\delta_1 i+\delta_2(L-i)]\tilde{g}(r)}-1\right)\right]dr} \tag{31}$$

In general a n-term sum of exponentials will result to an $(n-1)$-th order sum in (31). For systems with forward-error-control the complexity is even higher as shown in the next section.

B. Systems With Forward-Error-Control

Throughout this section it is assumed that no side information is available about the presence or absence of other-user interference.

Reed-Solomon Codes With Error-Correction

Let (n,k,m) be a Reed-Solomon code over $GF(2^m)$, which uses minimum distance error-correction decoding. Assuming that the m bits within the RS symbol suffer independent errors when conditioned on $(k_1,k_2,\ldots,k_J)$ (the number of users in each subregion which cause full hits). We can write for the probability of m bits [one symbol from $GF(2^m)$] being correct as

$$\tilde{P}_{c,s} = \left[1-Q\left[\frac{1}{\sqrt{x}}\right]\right]^m \geq \left[\frac{1+e^{-x}}{2}\right]^m ; \quad x \geq 0 , \tag{32}$$

for an AWGN channel, and

$$\tilde{P}_{c,s} = \left\{1-\frac{1}{2}\left[1-\frac{1}{\sqrt{1+x}}\right]\right\}^m \geq \sum_{l=1}^{3} c_l e^{\delta_l x}; \quad x \geq 0 , \tag{33}$$

for a Rayleigh nonselecting fading channel. In (33) c_l and δ_ls for $l = 1,2,3$ can be found as before (See Appendix). x is the same as the term inside the [ ] in (17), except that $E_{b,0}/N_0$ should be replaced by $\frac{k}{n}\cdot E_{b,0}/N_0$; similar modification is necessary for the Rayleigh fading case. Subsequently the probability of an RS codeword being correct [when conditioned on $(k_1,k_2,\ldots,k_J)$] is

$$\tilde{P}_C = \sum_{i=0}^{t} \begin{bmatrix} n \\ i \end{bmatrix} (1-\tilde{P}_{c,s})^i \; \tilde{P}_{c,s}^{n-i} = \sum_{i=0}^{t} \begin{bmatrix} n \\ i \end{bmatrix} \sum_{l=0}^{i} \begin{bmatrix} i \\ l \end{bmatrix} (-1)^l \tilde{P}_{c,s}^{n-i+l} \tag{34}$$

where $\tilde{P}_{c,s}$ is given by (32) or (33), and $t=(n-k)/2$ is the error-correcting capability of the code.

The next step involves computing the expectation of $\tilde{P_C}$ over the number of hits and distribution of users:

$$P_C = E_{\underline{K}}\{E_h\{\tilde{P}_C\}\} = \sum_{i=0}^{t} \begin{bmatrix} n \\ i \end{bmatrix} \sum_{l=0}^{i} \begin{bmatrix} i \\ l \end{bmatrix} (-1)^l E_{\underline{K}}\{E_h\{\tilde{P}_{c,s}^{n-i+l}\}\} \tag{35}$$

Because of the similarity of (28)-(30) and (32)-(33) the expected value in (35) can be shown to be $F(m[n-i+l])$, where the function $F(\cdot)$ is given by (31). The final result for the packet error probability is

$$P_E = 1-P_C = 1-\sum_{i=0}^{t} \begin{bmatrix} n \\ i \end{bmatrix} \sum_{l=0}^{i} \begin{bmatrix} i \\ l \end{bmatrix} (-1)^l F(m[n-i+l]), \tag{36}$$

where we assumed that one codeword is transmitted per packet.

Notice that for a n-term sum of exponentials used to bound $\tilde{P}_{c,s}$ in (32), P_E of (36) includes a n+1 order sum.

Once we compute the packet error probability, the expected throughput can be obtained by multiplying the average traffic load by the probability of success, as derived in [4]. Normalizing the throughput by the bandwidth expansion factor, we may write the normalized throughput, η, as:

$$\eta = \lambda S \; P_C \frac{1}{Nq} \frac{k}{n} m \tag{37}$$

in bits per slot per frequency. For the circular region of radius R, $S = \pi R^2$.

IV. CELLULAR RADIO NETWORKS WITH NONCOHERENT DS/SS OR FH-DS/SS SIGNALING

A. Systems Without Forward-Error-Control

For systems employing MFSK modulation with noncoherent demodulation, asynchronous users (at the dwell-time level) over an AWGN channel, the starting point is the following expression for the conditional M-ary symbol error probability (see [9]):

$$\tilde{P}_{e,s} = \sum_{m=1}^{M-1} \begin{bmatrix} M-1 \\ m \end{bmatrix} \frac{(-1)^{m+1}}{m+1} \exp\left\{-\frac{m}{2(m+1)\sigma_Z^2}\right\} \tag{38}$$

where we have conditioned on $(k_1, k_2, \ldots, k_J)$ and $(k_1', k_2', \ldots, k_J')$ [(k_j, k_j') $j=1,2,\ldots,J$ denote the number of mobile stations in region A_j that cause full and partial hits, respectively]. σ_Z^2 corresponds to the second-order moment of the decision variables $\tilde{Z}_{c,m}$ and $\tilde{Z}_{s,m}$. It is given by

$$\sigma_Z^2 = \left[\left(\frac{2E_{b,0}\log_2 M}{N_0} g(\bar{r})\right)^{-1} + \frac{m_\Psi}{MN} \sum_{j=1}^{J} \bar{g}(r_j)(k_j + \frac{k_j'}{2})\right]^{-1}$$

As in the last section, we have approximated the random variables $\tilde{Z}_{c,m}$ and $\tilde{Z}_{s,m}$ by zero-mean Guassian random variables with the same second-order moments. Let $\tilde{P}_{c,s} = 1 - \tilde{P}_{e,s}$ and use the three-term exponential bound to obtain

$$\tilde{P}_{c,s} = 1 - \sum_{m=1}^{M-1} \begin{bmatrix} M-1 \\ m \end{bmatrix} \frac{(-1)^{m+1}}{m+1} \exp\left\{-\frac{m}{2(m+1)x}\right\} \geq \sum_{l=1}^{3} c_l e^{\delta_l x} ; \tag{39}$$

where x denotes σ_Z^2. Define

$$\tilde{c_l} = c_l \exp\left\{\delta_l \left[\frac{2E_{b,0}\log_2 M}{N_0} g(\bar{r})\right]^{-1}\right\}, \tag{40}$$

and

$$\tilde{g}(r) = \frac{m_\Psi}{MN}\bar{g}(r)\,, \tag{41}$$

where m_Ψ is defined after eq. (22), and $\tilde{g}_j = \tilde{g}(r_j)$.

Following the same method as for proving (23) we obtain

$$E_K\{E_h\{\tilde{P}_{c,s}\}\} = \sum_{l=1}^{3} \tilde{c}_l\, e^{\lambda \sum_{j=1}^{J} S_j [P_f (e^{\delta_l \tilde{g}_j} - 1) + P_p (e^{\delta_l \frac{1}{2} \tilde{g}_j} - 1)]} \tag{42}$$

In (42) $P_f = \left[1 - \frac{1}{N_s}\right]\frac{1}{q}$ and $P_p = \frac{2}{N_s}\frac{1}{q}$ are the probabilities for full and partial hits, respectively, and $N_s = \frac{N_b}{\log_2 M}$ is the number of M-ary symbols per dwell-time. For a circular region with radius R we finally obtain

$$P_{e,s} = 1 - \sum_{l=1}^{3} \tilde{c}_l\, e^{\lambda \int_0^R 2\pi r [P_f (e^{\delta_l \tilde{g}(r)} - 1) + P_p (e^{\delta_l \frac{1}{2} \tilde{g}(r)} - 1)] dr} \tag{43}$$

For Rayleigh nonselective fading (38) should be replaced by

$$\tilde{P}_{c,s} = 1 - \sum_{m=1}^{M-1} \begin{bmatrix} M-1 \\ m \end{bmatrix} \frac{(-1)^{m+1}}{m+1+m\,\sigma_Z{}^2} \geq \sum_{l=1}^{3} c_l\, e^{\delta_l \sigma_Z{}^2}\,,$$

where $\sigma_Z{}^2$ is now given by

$$\sigma_Z{}^2 = \left[\left[\frac{\bar{E}_b \log_2 M}{N_0} g(\bar{r})\right]^{-1} + \frac{m_\Psi}{MN}\sum_{j=1}^{J}\bar{g}(r_j)(k_j + \frac{k_j'}{2})\right]^{-1}$$

and $P_{e,s}$ is still given by (43), where now

$$\tilde{c}_l = c_l \exp\left\{\delta_l \left[\frac{\bar{E}_{b,0} \log_2 M}{N_0} g(\bar{r})\right]^{-1}\right\} \tag{44}$$

To evaluate the **packet error probability** for uncoded systems we proceed as we did for the corresponding case of Section III.A (eq. (28)-(31)). The result corresponding to (31) is now

$$P_C = G(L) = \sum_{i_1=0}^{L} \binom{L}{i_1} \sum_{i_2=0}^{L-i_1} \binom{L-i_1}{i_2} \bar{c}_1^{\,i_1} \bar{c}_2^{\,i_2} \bar{c}_3^{\,L-i_1-i_2} \exp\left\{ \lambda \int_0^R 2\pi r \left[P_f \left(e^{[\delta_1 i_1+\delta_2 i_2+\delta_3(L-i_1-i_2)]\bar{g}(r)} - 1 \right) + P_p \left(e^{\frac{1}{2}[\delta_1 i_1+\delta_2 i_2+\delta_3(L-i_1-i_2)]\bar{g}(r)} - 1 \right) \right] dr \right\} . \quad (45)$$

For the special case of binary FSK ($M = 2$), (39) reduces to

$$\tilde{P}_{c,s} = 1 - \frac{1}{2} e^{-1/4x} \quad . \quad (46)$$

Using the exponential bound of (18), we get the lower bound on $\tilde{P}_{c,s}$ as

$$\tilde{P}_{c,s} \geq \frac{1}{2} + \frac{1}{2} e^{-2x} \quad . \quad (47)$$

Using bound of (47) reduces the expression in (45) to a single sum where now $c_1 = c_2 = \frac{1}{2}$, and $\delta_1 = 0, \delta_2 = -2$. In order to validate the tightness of (47) for BFSK systems, we evaluated the exact bit error probability for BFSK frequency-hopped systems under the assumption of full hits. The conditional bit error probability in this case is given by [11]

$$P_b(\underline{K}) = \int_0^\infty \exp\left\{ -\frac{N_0 u^2}{2E_{b,0}\bar{g}(\bar{r})} \right\} J_0(u)\, \Phi(\underline{K},u)\, du \quad , \quad (48)$$

where we have conditioned on $\underline{K} = (K_1, K_2, \ldots, K_J)$; K_i being the number users causing full hits from region A_i. $\Phi(\underline{K},u)$ is given by

$$\Phi(\underline{K},u) = \prod_{i=1}^{J} \left[1 - P_h + P_h J_0(u\sqrt{\bar{g}_j}) \right]^{K_i} \left\{ \sum_{i=1}^{J} \frac{K_i \sqrt{\bar{g}_i} P_h J_1(u\sqrt{\bar{g}_i})}{2[1 - P_h + P_h J_0(u\sqrt{\bar{g}_i})]} + \frac{uN_0}{2E_{b,0}\bar{g}(\bar{r})} \right\} ;$$

$J_n(.)$ is the Bessel function of the first kind of order n and $P_h = P_p + P_f$. Taking the expectation with respect to $\underline{K}$ as in section III results in

$$\Phi(u) = \exp\left\{\lambda P_h \int_0^R 2\pi r \left[J_0\left(u\sqrt{g(r)}\right) - 1\right]dr\right\} \left[\frac{uN_0}{2E_{b,0}g(\bar{r})} + \frac{\lambda P_h}{2} \int_0^R 2\pi r \sqrt{g(r)} J_1\left[u\sqrt{g(r)}\right] dr\right] \quad (49)$$

Substitution of (49) into the integral of (48) gives the desired result.

B. Systems With Forward-Error-Control

Just as in Section III.B it is assumed that no side information about the presence of the other-user interference is available.

Reed-Solomon Codes With Error-Correction

Consider (n,k,m) Reed-Solomon codes over $GF(M^m)$ with minimum distance error-correction decoding. Assume that one RS symbol per dwell time and one codeword per packet are transmitted. As before, we multiply the signal-to-noise ratio factor by the code rate to account for the error control reduction in the energy per information symbol.

The rest of the analysis follows closely that of Section III.B for RS codes. Equations (34)-(35) are still valid. In Eq. (36), we only need to replace $F(m[n-i+l])$ by $G(m[n-i+l])$ which is now given by (45). Multiplying the expression in (37) by $\log_2 M$ gives the throughput in bits per slot per frequency.

V. NUMERICAL RESULTS

As we mentioned earlier, we take the cell area to be a circular region of radius R. In all the subsequent results, we have set $R = 1$ and $r_0 = 0.01R = 0.01$. This can be viewed as a normalization. The normalization is in the sense that, in the mobile-to-base mode of operation, all mobiles transmit with the signal-to-noise ratio, E_b/N_0, such that the SNR received at the base from a mobile at the periphery of the cell, given by $\overline{E_b/N_0} = (E_b/N_0)g(R)$, is greater than minimum SNR required for reliable communication. Therefore, if $\overline{E_b/N_0}$ is set at the minimum acceptable level for reliable communication, the transmitted SNR for all mobiles is given by $E_b/N_0 = (\overline{E_b/N_0})/g(R)$; if $R = 1$, $E_b/N_0 = \overline{E_b/N_0}$, while if $R > 1$, $g(R)$ can be computed and used to determine E_b/N_0 from the above formula. Therefore, using $R = 1$, the expected number of users in A is given by $\overline{K} = \lambda\pi R^2 = \lambda\pi$; hence our results are indexed by $\overline{K}$.

All the throughput results are shown in terms of normalized throughput η, in bits/slot/frequency. Normalization by the bandwidth expansion factor and the presentation of throughput in terms of number of bits per slot rather than packets per slot allows the fair comparison of all systems considered.

Figure 2. compares the exact evaluation of bit error probability for a DS/SS system (eq. (10)) with the bound on the Guassian approximation of the same quantity (eq. (19)-(24)). An important observation is the fact that although we have bounded an approximation of the desired quantity, we have obtained a bonafide bound on the true value of the bit error probability. This bound is rather loose for small number of active users, but becomes tight as the number of users increases. We have delibrately shown the results for $P_b > 10^{-2}$ to observe the tightness of the bound for very large number of users.

Figure 3a. presents the throughput of a Hybrid system and compares the performance of coded and uncoded systems. It is observed that coding improves the throughput in bits/slot/frequency significantly. Figure 3b. shows the packet error probability for the same system. This Figure includes the packet error probabilities of greater than 10^{-1} to illustrate the fact that maximum throughput is acheived at high error rates. The coded system also has a better packet error performance. For the coded system, the maximum throughput of 9 (bits/slot/frequency) is acheived at $P_E = 0.5$. Certainly, this is not an acceptable error rate for reliable communication. When we impose a limit on the maximum allowable error rate, we acheive reliable communication at the cost of lower throughput. This point has been discussed also in [2]. In all subsequent results, we show the throughput for packet error probabilities of less than 10^{-1}. This is the operating region of interest in most practical systems.

Figures 4a.-4b. illustrate the throughput and packet error rate of frequency-hopped, Hybrid, and direct-sequence systems. It is observed that FH system performs best both in terms of throughput and error rate, while the pure DS system has the worst performance among the above systems. This result is opposite of the case where we do not take into account the effect of varying received power. In the case where the received power is assumed to be constant for all users (i.e., $g(r) = 1$), the direct-sequence system performs best in a Multiple-Access environment. This result is validated in [6], and can be seen in Figure 5., where we compare the bit error probabilities for the case that received power is constant and when we take into account the effect of varying power. We assumed that all users are at distance $\bar{r}$ from the base station. This behavior can be traced to the near-far problem in spread-spectrum communication systems in which the direct-sequence systems experience severe degradation in performance, while in frequency-hopped systems, this problem is not as dominant and the performance degrades rather gracefully.

Figures 6a.-6b. illustrate the throughput and packet error rate for three different values of code rate. It is observed that for small number of users ($\bar{K} \leq 400$), the rate 1/2 code has the best performance in terms of packet error probability, while the rate 1/4 code does better for $\bar{K} > 400$. Higher rate codes always do better in terms of throughput. Again if we impose a constraint on the maximum allowable error rate of a given scheme, there exists a best code rate for a given number of users.

Figures 7. presents similar result in Rayleigh nonselective fading environment. Figure 8. shows the performance of non-coherent 32-ary FSK modulation system for different values of spreading parameters. Notice that all the systems look to perform the same for $\bar{K} < 300$. This is due to the fact that the probability of packet errors were so small for $\bar{K} < 300$ that when we multiply the offered load by the success probability, the differences are practically negligible.

Figure 9. compares the bound on the bit error probability of a frequency-hopped BFSK system with the exact evaluation of this quantity. As in the DS system case, the bound over the Guassian approximation is a bonafide bound on the exact value of the bit error probability. Unlike the DS system, this bound is rather uniformly tight for all values of $\bar{K}$. Figures 10a.-10b. present the throughput and packet error rate for BFSK non-coherent systems for different values of code rate. Again the higher rate code does better in terms of throughput, but there exists an optimal code rate when one considers the constraint on the error rate. Figure 11. shows the performance of a Hybrid BFSK system for different values of spreading parameters. Again, the pure FH system does best, while the pure DS system performs worst due to the near-far problem.

VI. CONCLUDING REMARKS

We presented methods to obtain bounds on the bit and packet error probabilities of Hybrid DS-SFH/SS systems and use the results to evaluate the throughput in bits/slot/frequency of aformentioned systems. The method was based on the bounding of error probabilities by sum of exponentials. Although, we derived the bounds on the Guassian approximations of relevant quantities, the comparison of bounds with their exact counterpart shows that the derived bounds are valid for all systems of interest.

Another observation was the significant improvement of both throughput and packet error performance of coded systems over uncoded ones. It was also observed that under constraint of maximum allowable error rate, optimal code rates exist for a given system and number of users in the network. The near-far problem in spread-spectrum systems was vividly quantified and evident in our numerical results. It was concluded that under the realistic assumption of varying received power as a function of distance, the frequency-hopped system does best among all the systems considered. Hybrid systems do almost as well as frequency-hopped systems in terms of throughput, but the error rate performance of pure FH systems is much better than Hybrid and pure DS systems. Non-coherent systems behave similarly and except for the loss due to non-coherent detection, no other significant changes was observed.

One final point to mention, concerns the computational complexity of the expressions. For example, we only considered the two and three-term exponential bound of probability of correct reception. This gives us an acceptable level of accuracy in our computations, however had we used larger term bounds, we would have gained little improvement compared to the price we would have paid for computational complexity of the relevant expressions.

VII. APPENDIX

In this Appendix, the coefficients in the three-term exponential bounds of probability expressions for 32-ary non-coherent FSK system and coherent BPSK system over Rayleigh fading channel are given. We used the DATAPLOT software package to generate these coefficients for the region of interest. The general form of bound is given by

$$P_c(x) \geq \sum_{i=1}^{3} c_l \, e^{\delta_l x}$$

The range of x, which was of interest to us is $0 \leq x \leq 2$. This is the interval in which the values of P_c are of interest. The coefficients were computed in order to obtain tight bounds in the given interval (See also Figure 1.).

Here are the coefficients, c_l and δ_l for the expressions used in previous sections:

1. Coherent BPSK over RAYLEIGH nonselective fading channel with RS code over GF(2^5) (eq. (33)):

$$c_1 = 0.464377 \qquad \delta_1 = -1.25488$$

$$c_2 = 0.113090 \qquad \delta_2 = -2.44651$$

$$c_3 = 0.422533 \qquad \delta_3 = -0.95564$$

2. Non-coherent 32-ary FSK over AWGN channel (eq. (39)):

$$c_1 = 0.3434022 \qquad \delta_1 = -5.23148$$

$$c_2 = 0.5348523 \qquad \delta_2 = -5.23613$$

$$c_3 = 0.1217455 \qquad \delta_3 = -0.3.59411$$

REFERENCES

[1] Verhulst, D., Mouly, M., and Szpirglas, J., "Slow Frequency Hopping Multiple Access for Digital Cellular Radiotelephone," *IEEE Journal on Selected Areas in Communications*, Vol. SAC-2, No. 4, July 1984.

[2] Pursley, M., "Frequence-Hop Transmission for Satellite Packet Switching and Terrestrial Packet Radio Networks," *Transactions on Information Theory*, Vol. IT-32, pp. 652-667, September 1986.

[3] Geraniotis, E., and Pursley, M., "Error Probabilities for Slow-Frequency-Hopped Spread-Spectrum Multiple-Access Communications over Fading Channels," Special Issue on Spread-Spectrum Communications of the *IEEE Transactions on Communications*, Vol. COM-30, pp. 996-1009, May 1982.

[4] Gluck, J. W., and Geraniotis, E., "Throughput and Packet Error Probability of Cellular Frequency-Hopped Spread-Spectrum Radio Networks," *IEEE Journal on Selected Areas in Communications*, Vol. SAC-7, No. 1, January 1989.

[5] Geraniotis, E., and Pursley, M., "Error Probability for Direct-Sequence Spread-Spectrum Multiple-Access Communications --Part II: Approximations," *IEEE Transactions on Communications*, Vol. COM-30, pp. 985-995, May 1982.

[6] Geraniotis, E., "Performance of Direct-Sequence Spread-Spectrum Multiple-Access Communications with Random Signature Sequences," Univ. of Massachusetts, Electr. and Comp. Engin. Report UMAS-ECE-OCT84-1, submitted to the *IEEE Transactions on Communications*, 1986.

[7] Geraniotis, E., "Coherent Hybrid DS/SFH Spread-Spectrum Multiple-Access Communications," Special Issue on Military Communications of the *IEEE Journal on Selected Areas in Communications*, Vol. SAC-3, pp. 695-705, September 1985.

[8] Geraniotis, E., "Performance of Noncoherent Direct-Sequence Spread-spectrum Multiple-Access Communications," Special Issue on Military Communications of the *IEEE Journal on Selected Areas in Communications*, Vol. SAC-3, pp. 687-694, September 1985.

[9] Geraniotis, E., "Noncoherent Hybrid DS/SFH Spread-Spectrum Multiple-Access Communications," *IEEE Transactions on Communications*, Vol. COM-34, pp. 862-872, September 1986.

[10] Hildebrand, F. B., *Introduction to Numerical Analysis*, New York, McGraw-Hill, 1956.

[11] Geraniotis, E., "Multiple-Access Capability of Frequency-Hopped Spread-Spectrum Revisited: An Exact Analysis of the Effect of Unequal Power Levels," Submitted to *IEEE Transactions on Communications*, 1988.

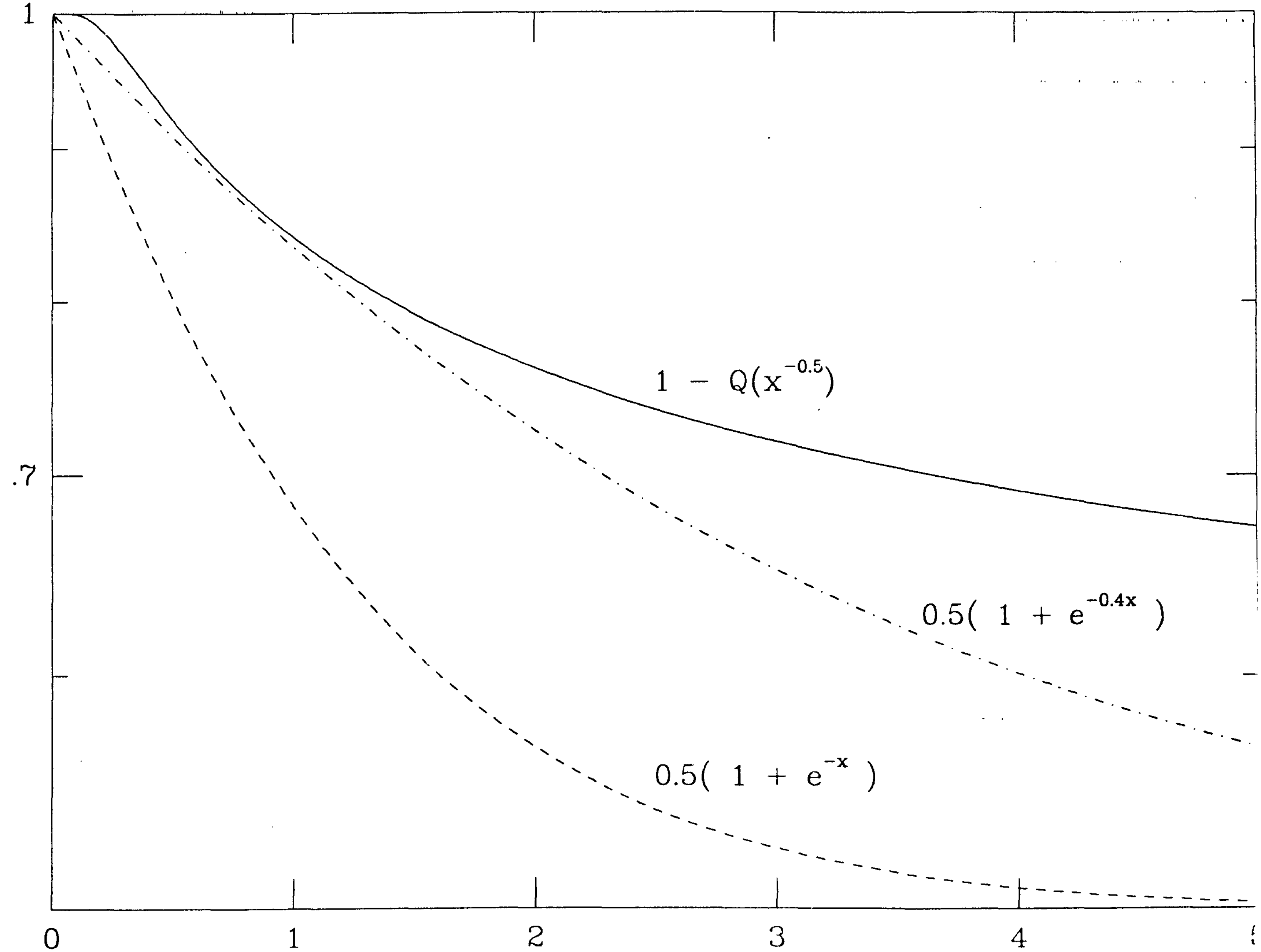

Figure 1. The bound of EQ.(19) along with the improved bound.

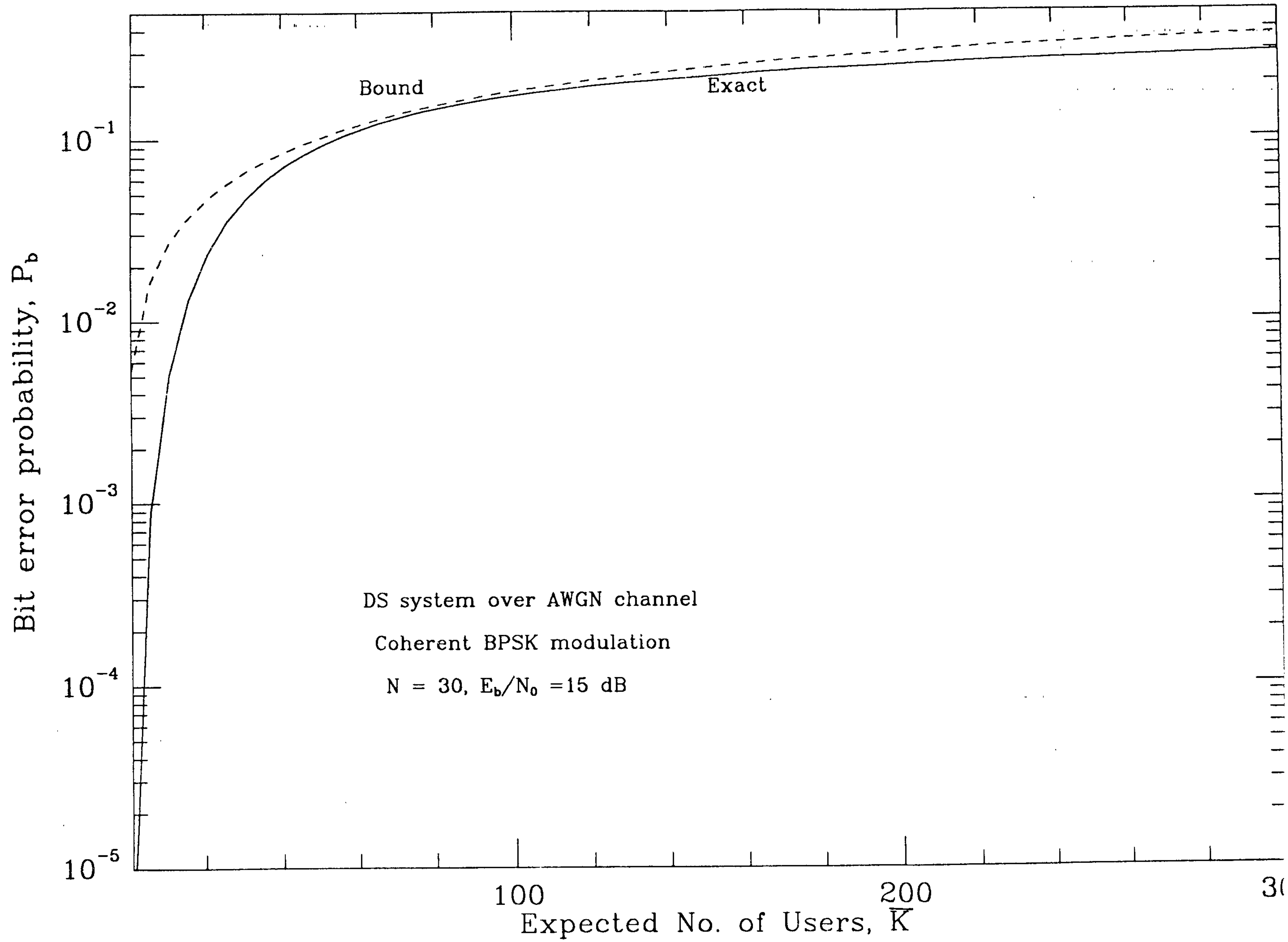

Figure 2. Comparison of the exact bit error probability with the bound of EQ.(19).

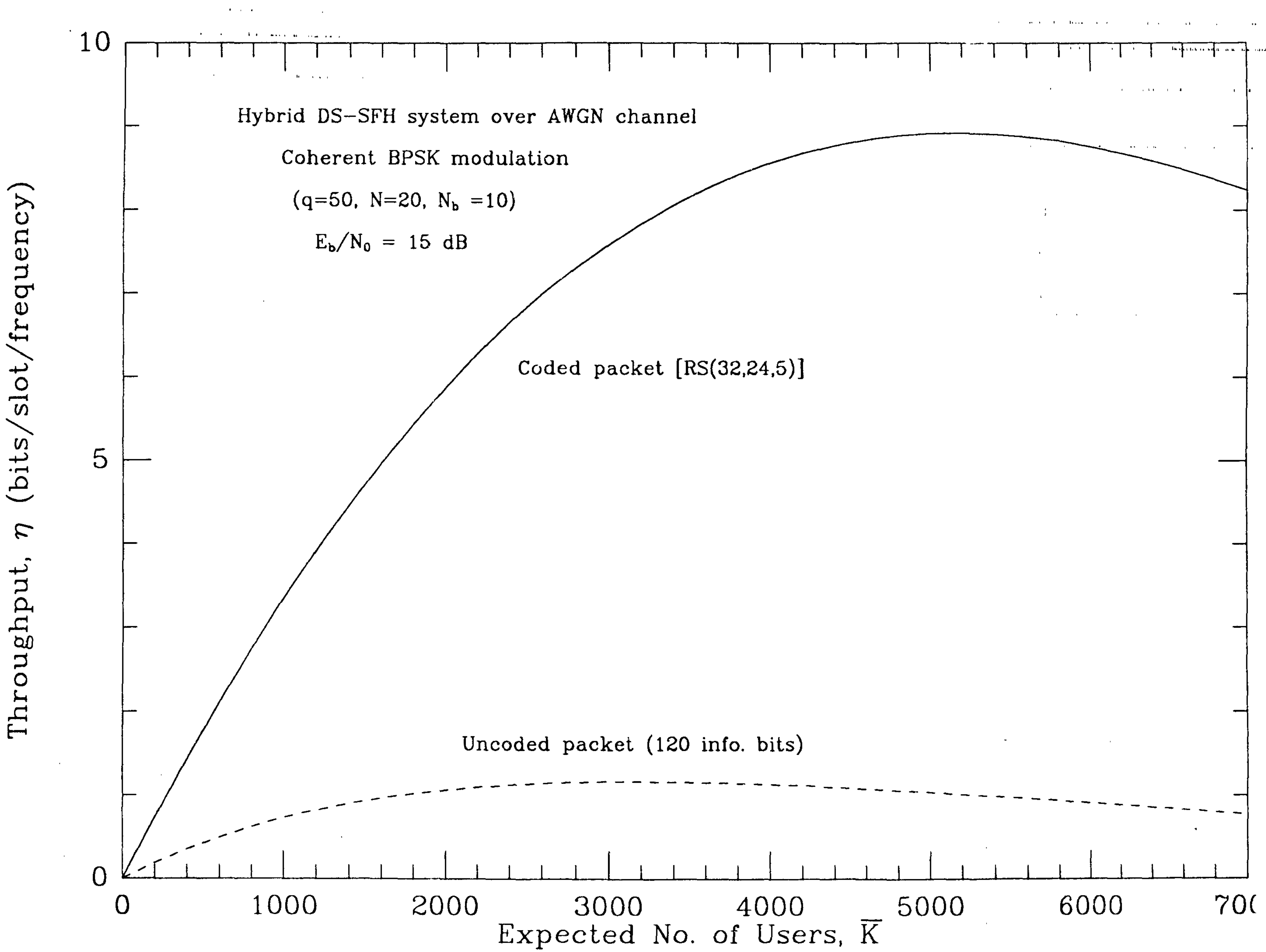

Figure 3a. Throughput vs. Average Number of Users for Coded and Uncoded systems.

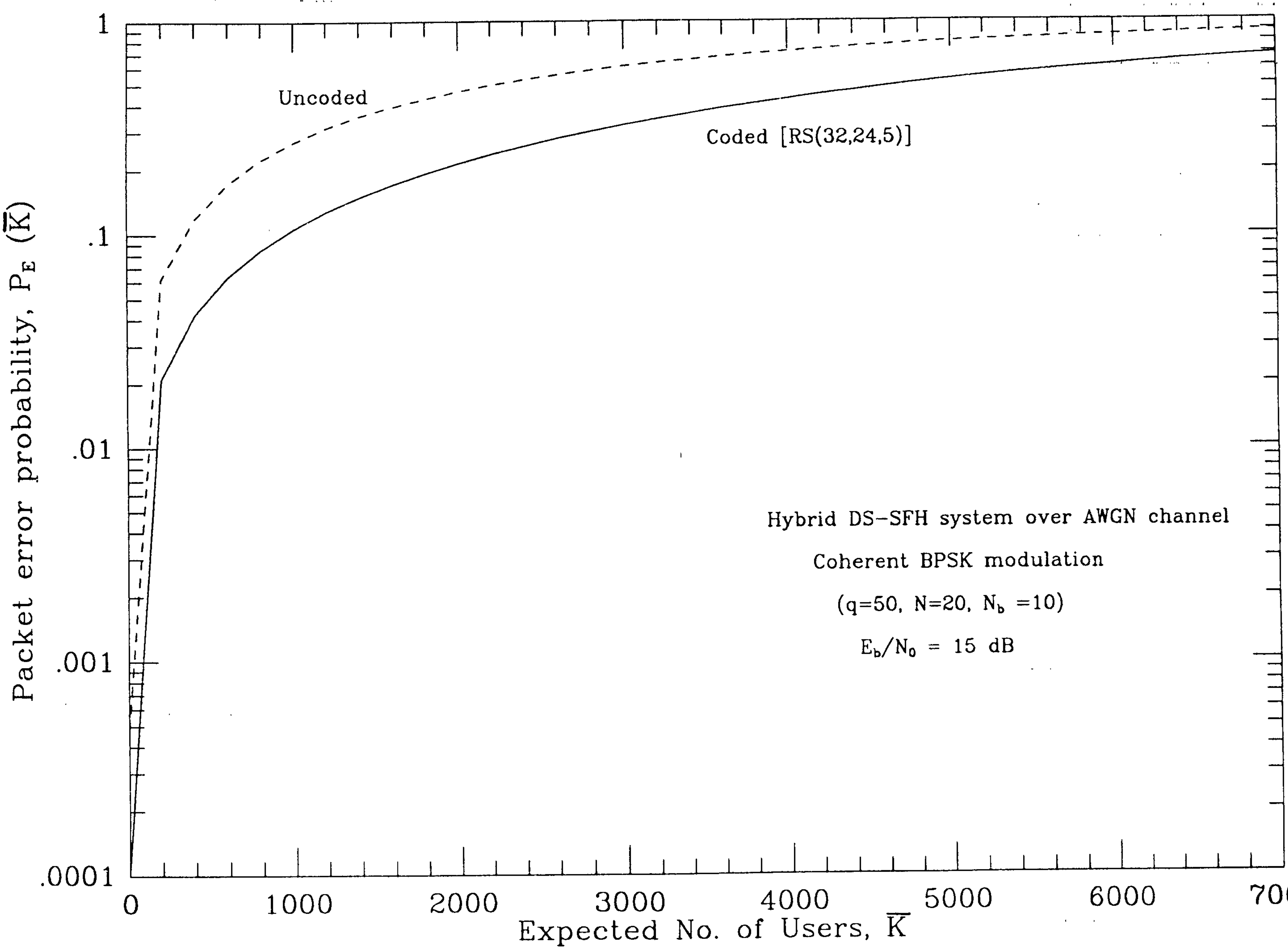

Figure 3b. Packet error probability vs. Average Number of Users for Coded and Uncoded systems.

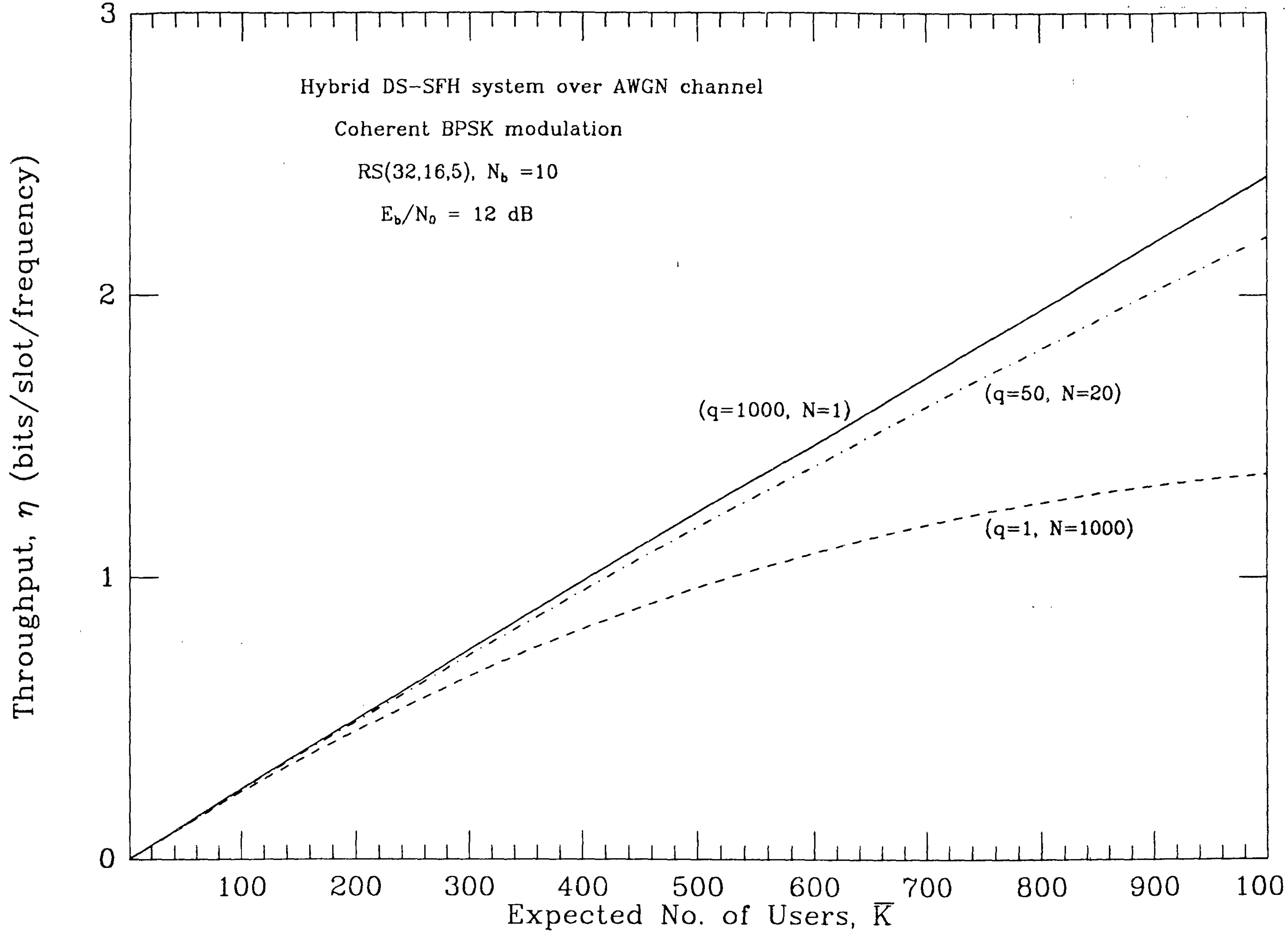

Figure 4a. Throughput vs. Average Number of Users for different values of spreading parameters.

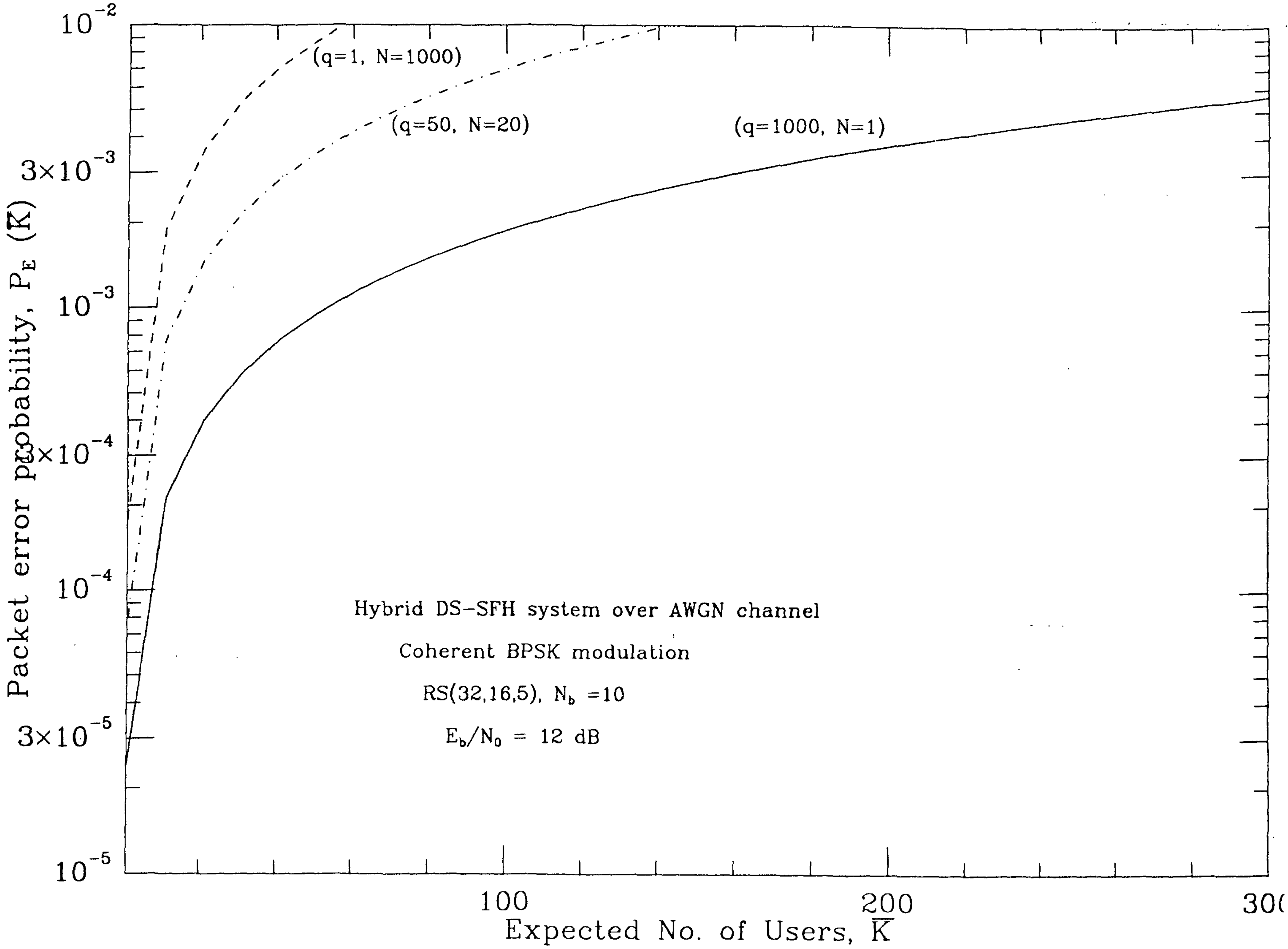

Figure 4b. Packet error probabilities for systems of Figure 4a.

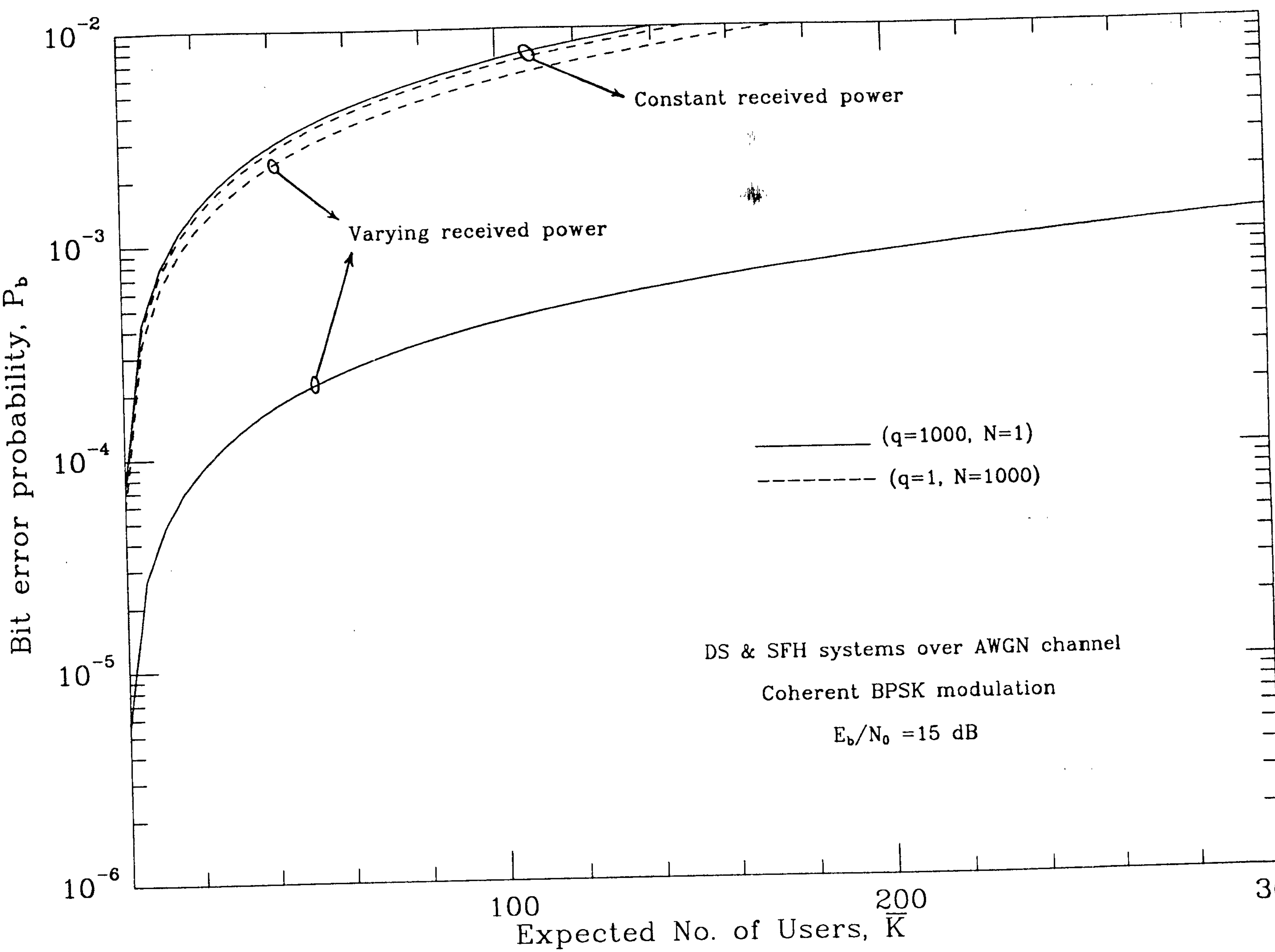

Figure 5. Comparison of bit error probability of DS and FH systems under the assumption of constant received power and varying received power.

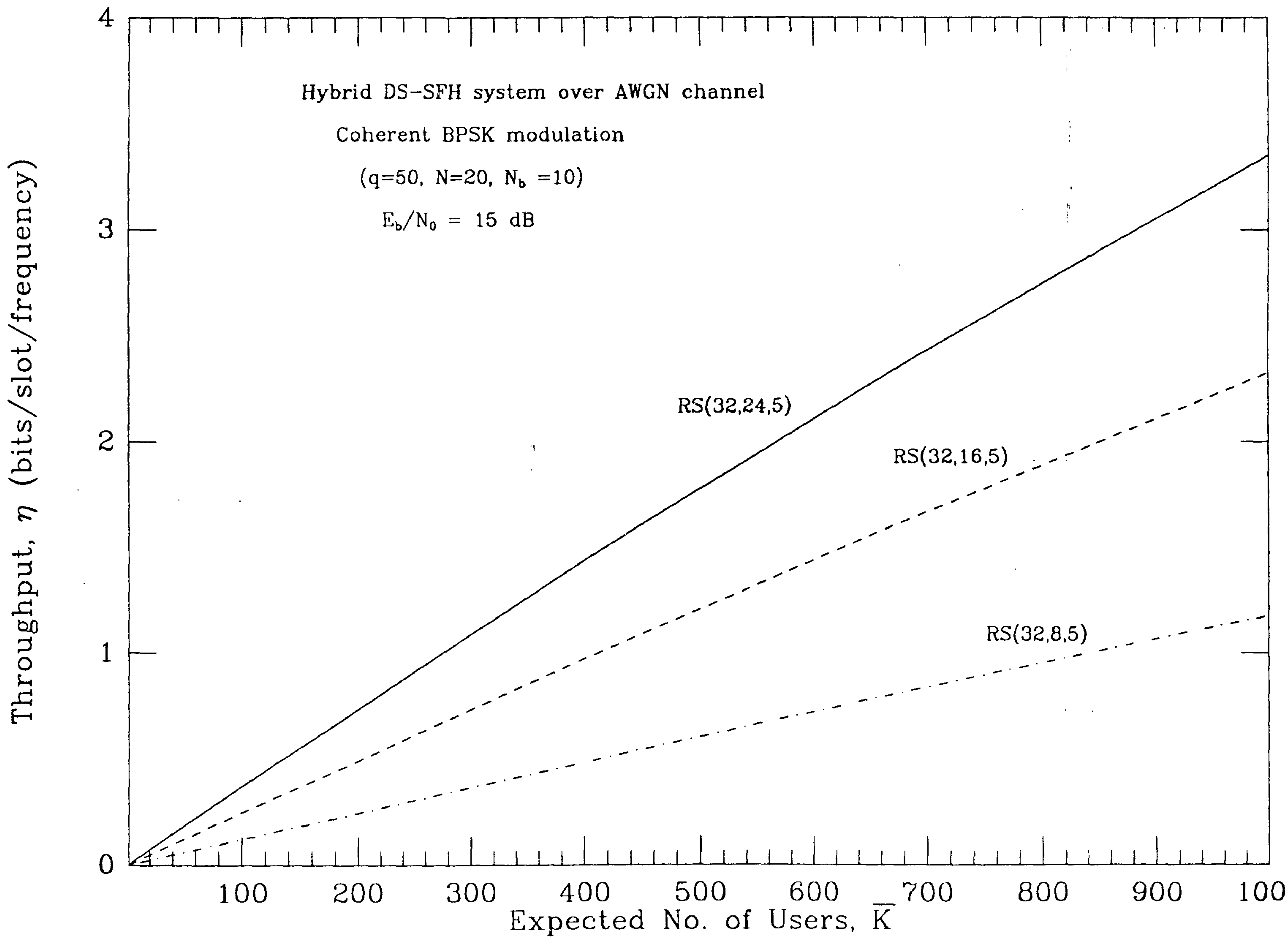

Figure 6a. Throughput for different values of code rate.

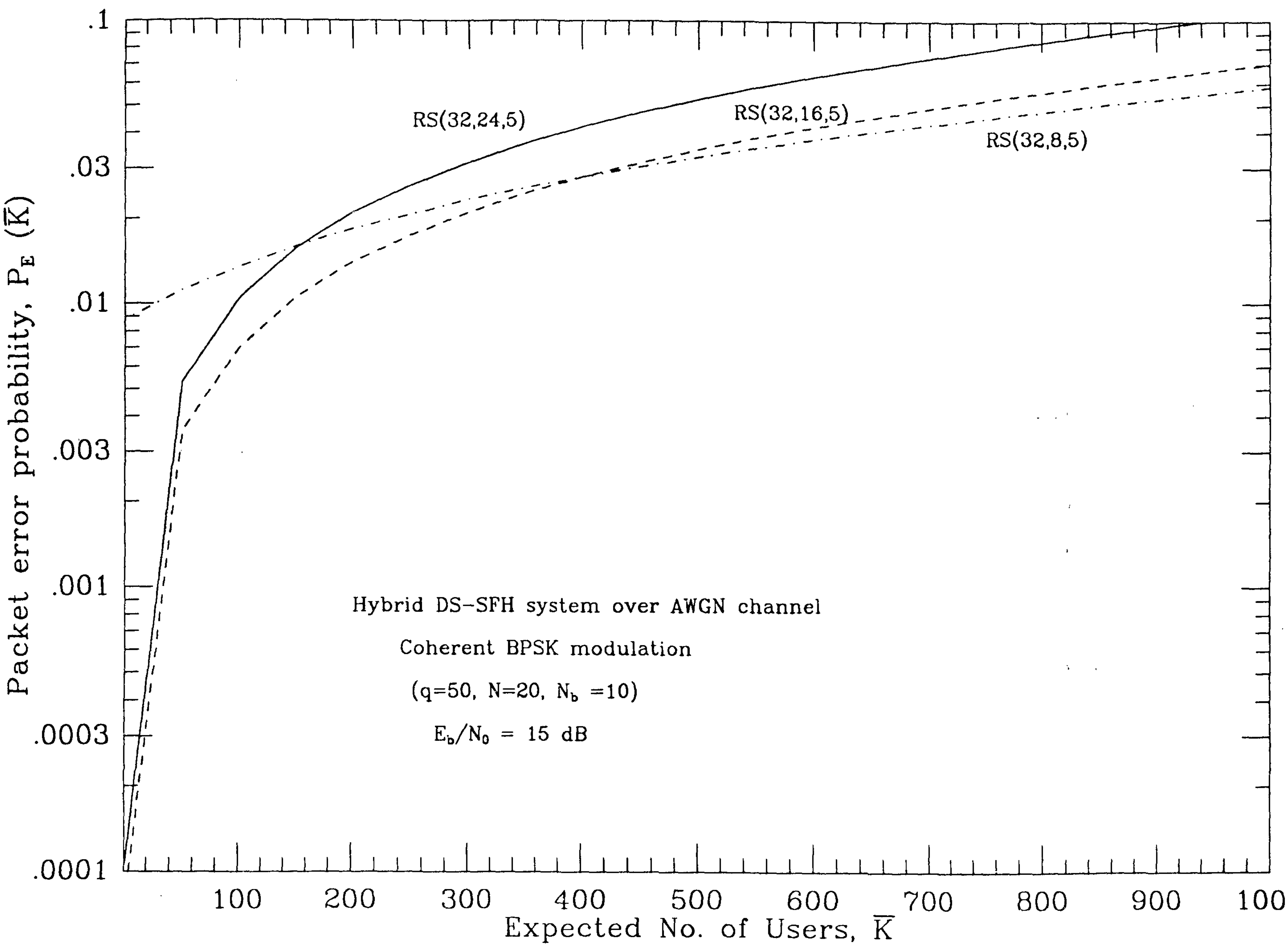

Figure 6b. Packet error probabilities for systems of Figure 6a.

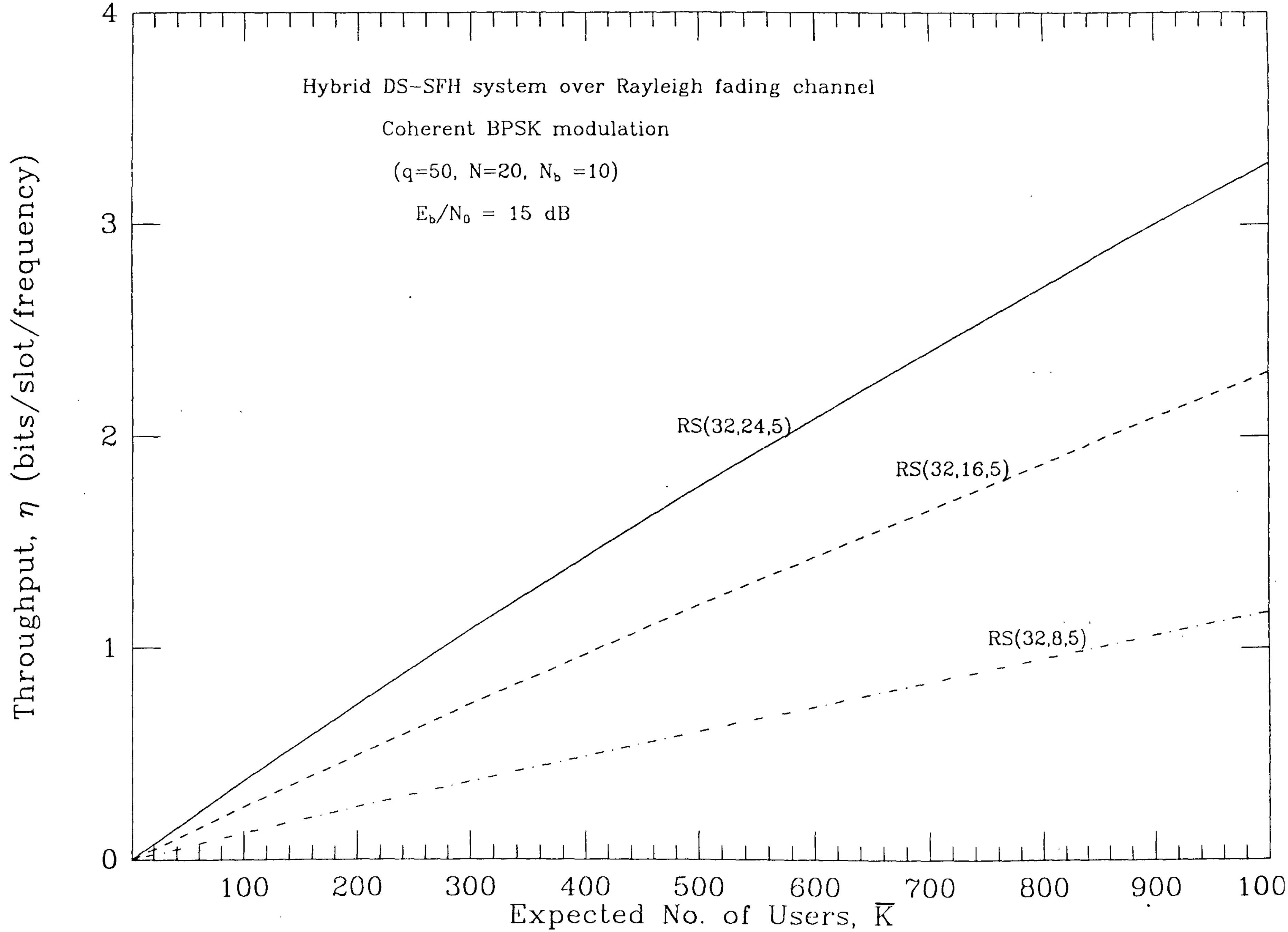

Figure 7. Throughput for different code rates over Rayleigh fading channel.

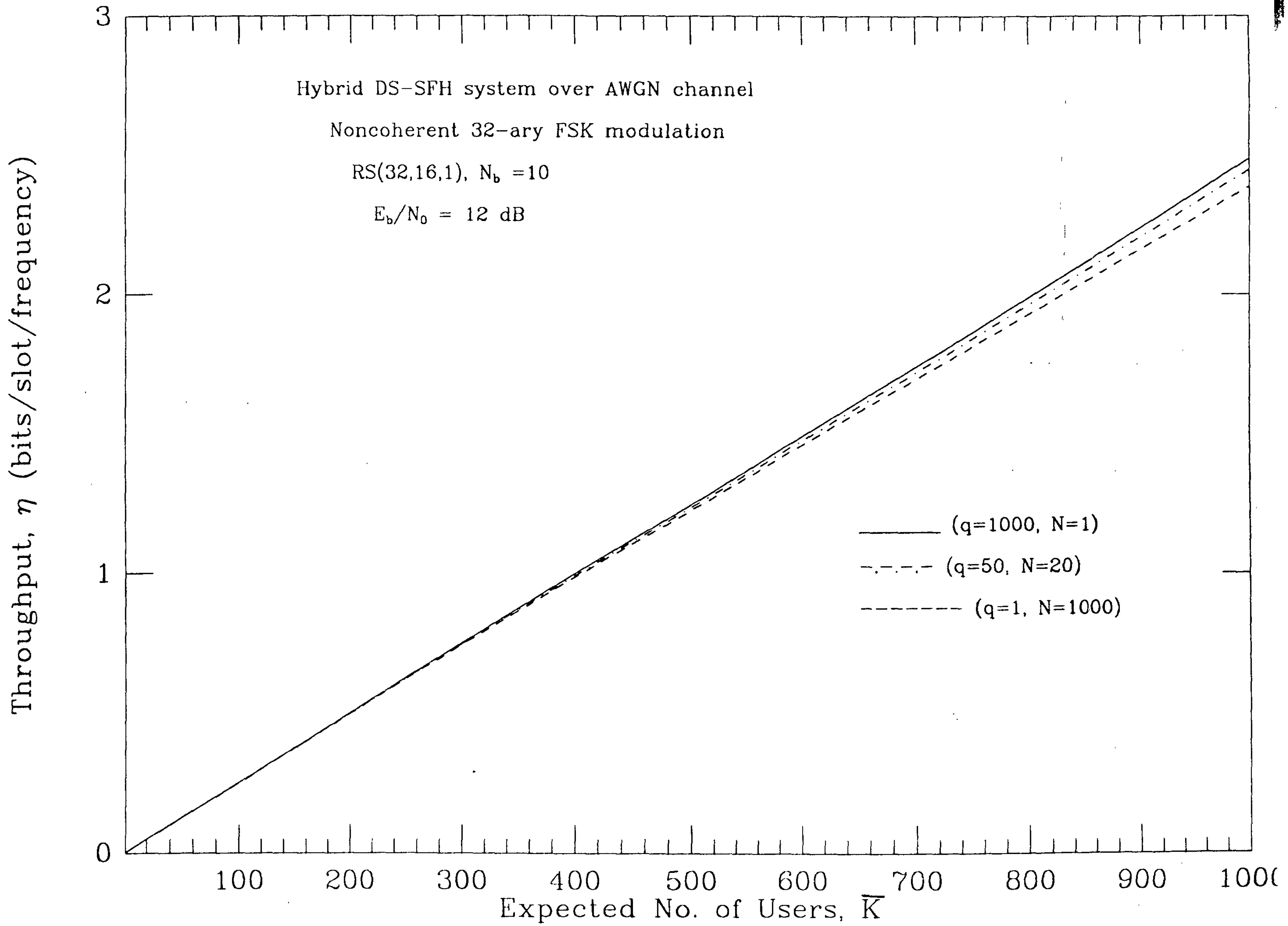

Figure 8. Throughput for 32-ary FSK system with different spreading parameters.

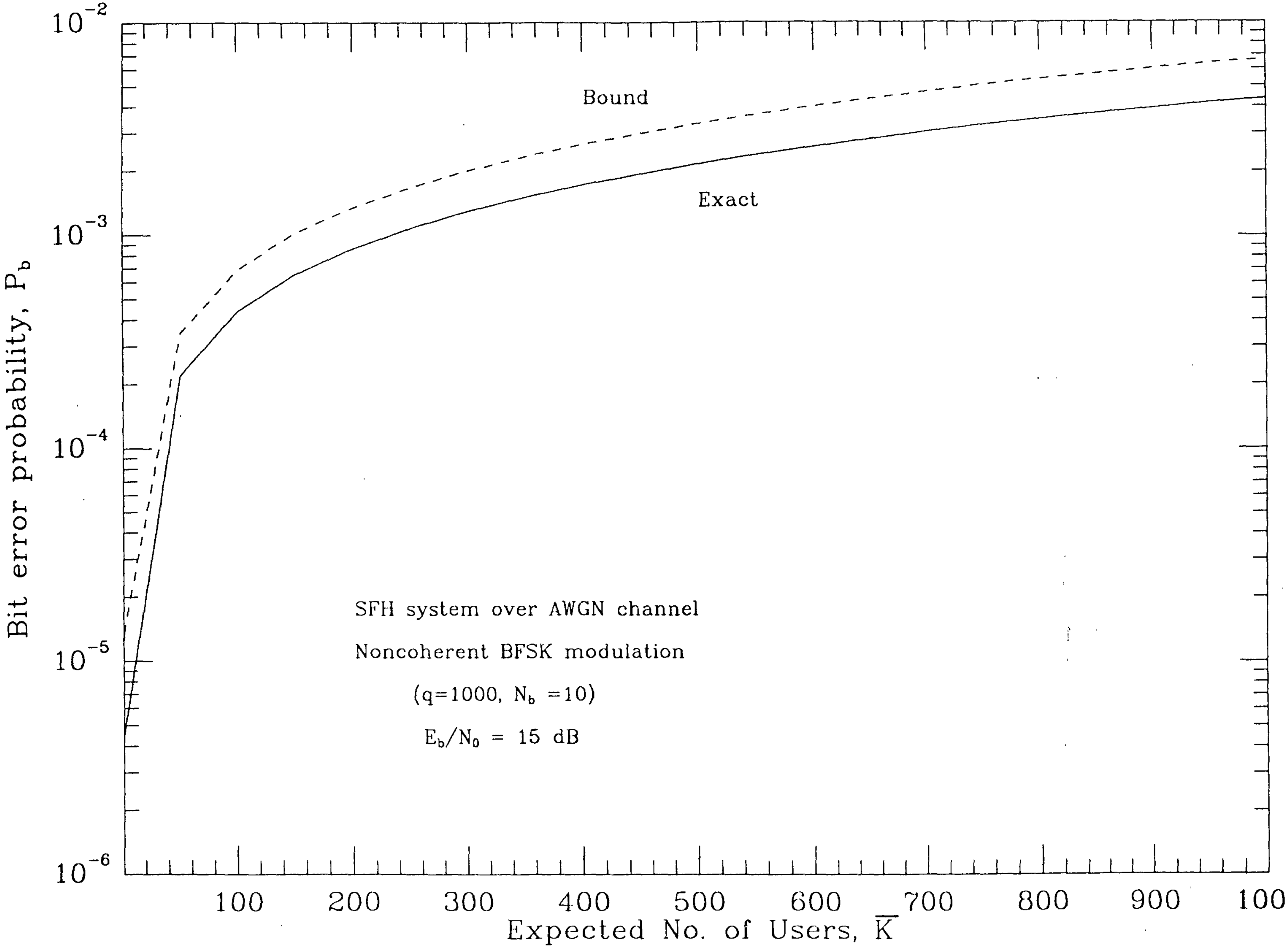

Figure 9. Comparison of exact bit error probability of Frequency-Hopped BFSK system with the bound of EQ.(47).

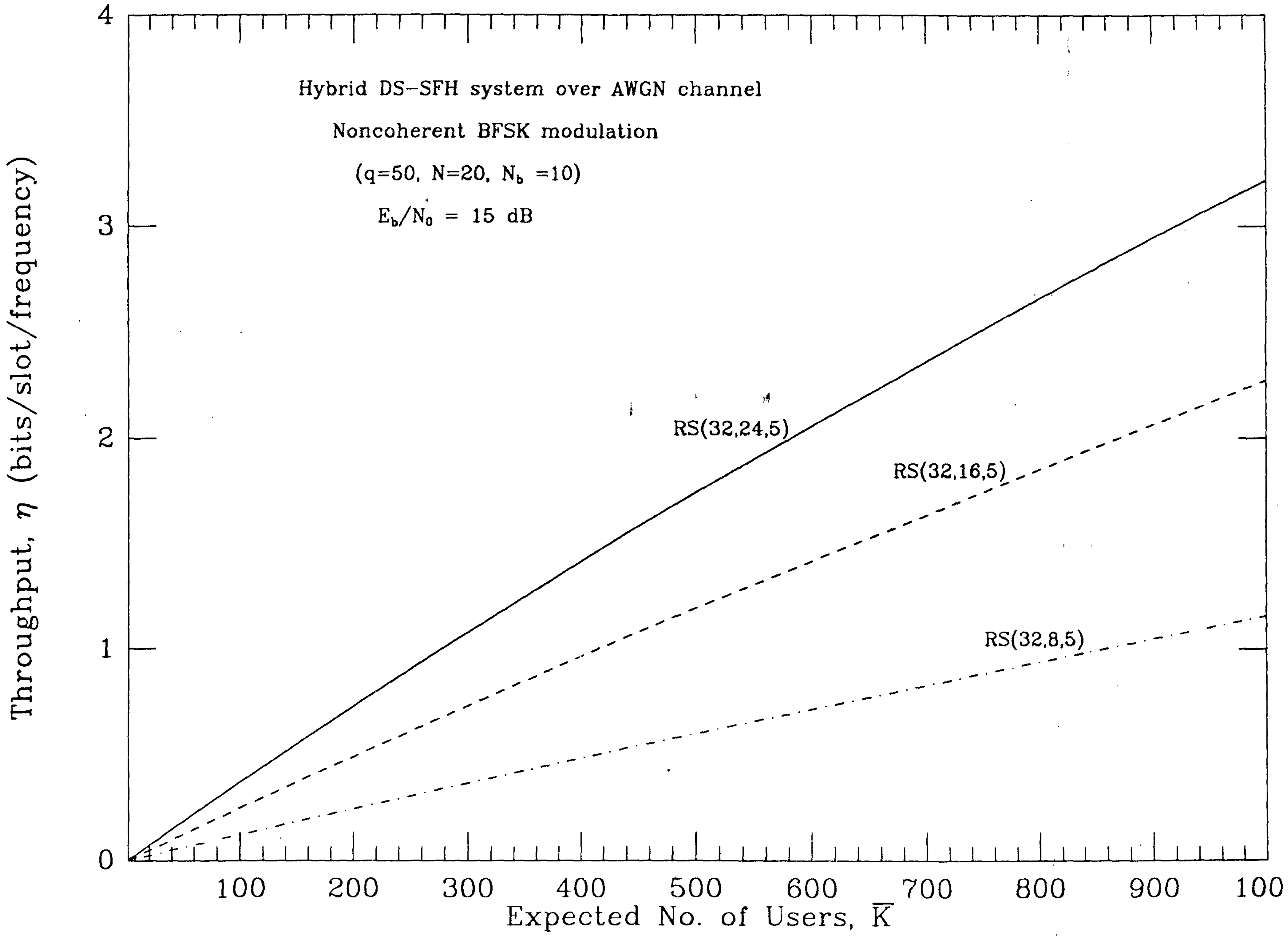

Figure 10a. Throughput for different code rates of Hybrid BFSK system.

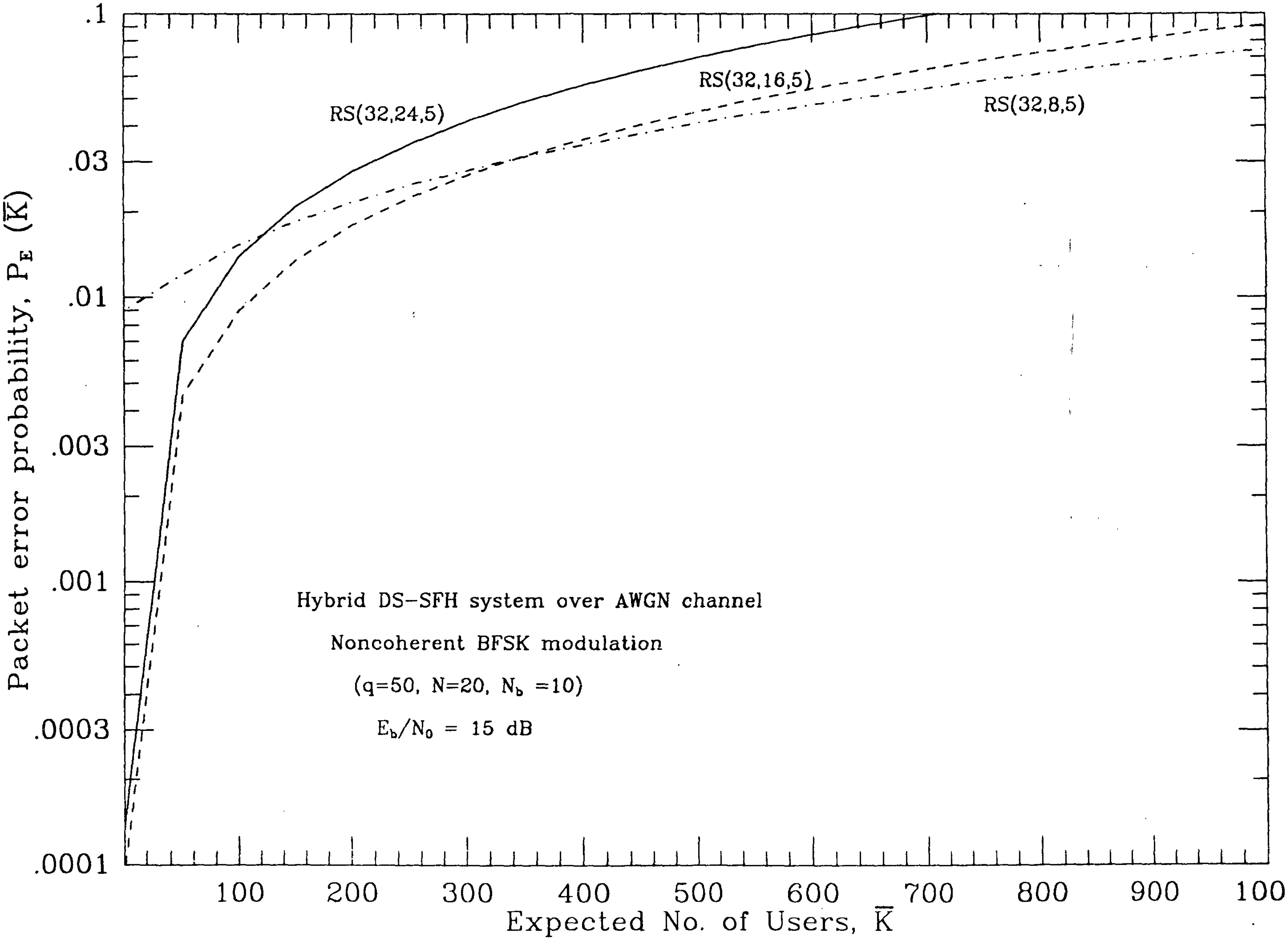

Figure 10b. Packet error probabilities for systems of Figure 10a.

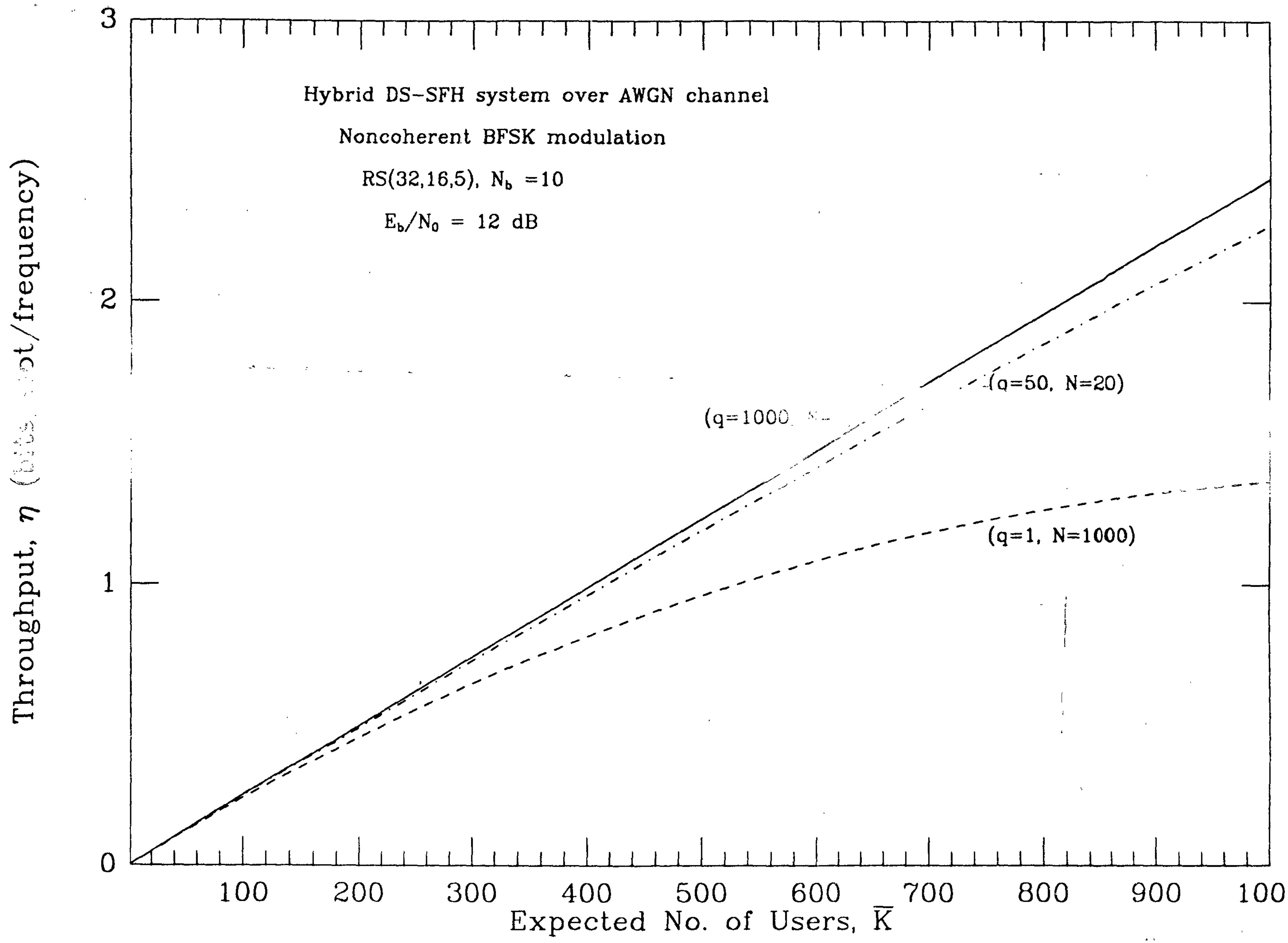

Figure 11. Throughput of Hybrid BFSK systems for different values of spreading parameters.

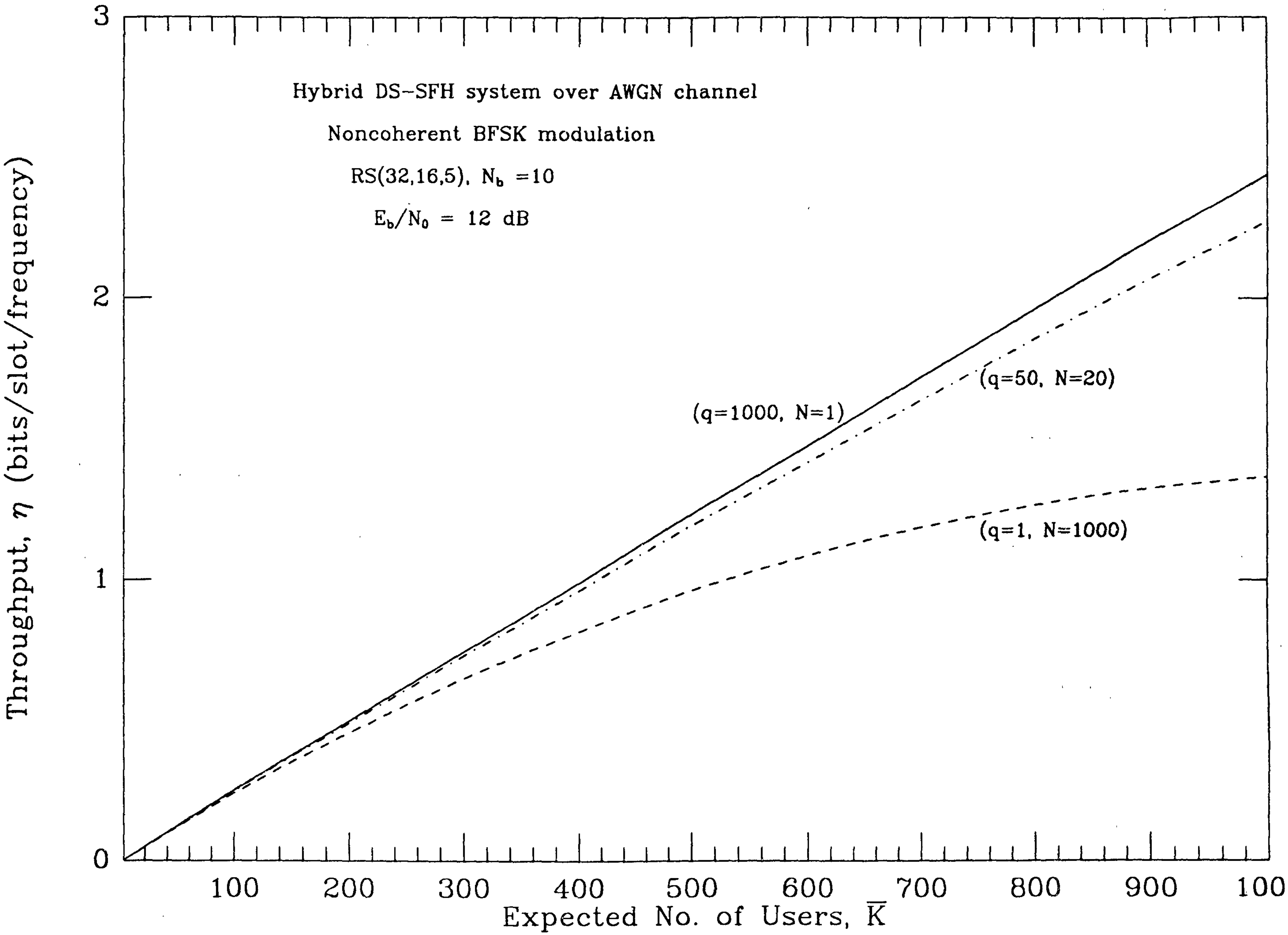

Figure 11. Throughput of Hybrid BFSK systems for different values of spreading parameters.